 Bull. Chem. Soc. Jpn. Vol. 80, No. 2, 371–386 (2007)

Orientation and Substituent Effects on the Properties of the Diacetylene-Group Connected Octaethylporphyrin–Dihexylbithiophene Derivatives (OEP–DHBTh–X) Carrying Electron-Withdrawing Groups#

Naoto Hayashi,[1] Takashi Nishihara,[1] Takuya Matsukihira,[1] Hiroki Nakashima,[1] Keiko Miyabayashi,[2] Mikio Miyake,[2] and Hiroyuki Higuchi*[1]

[1]Graduate School of Science and Engineering, University of Toyama, 3190 Gofuku, Toyama 930-8555

[2]School of Material Science, JAIST (Hokuriku), 1-1 Asahi-dai, Tatsunokuchi, Noumi, Ishikawa 923-1292

Received June 21, 2006; E-mail: higuchi@sci.u-toyama.ac.jp

Orientational isomers of the octaethylporphyrin–dihexylbithiophene (OEP–DHBTh) derivatives connected with a diacetylene linkage were synthesized, with various electron-withdrawing substituents X attached at the ends. The effects of DHBTh orientation and X substituent on the properties of OEP–DHBTh–X (X = H, Br, CN, CHO, and NO_2) were studied and compared with those of related OEP derivatives.

Previously, we reported the properties of the extended conjugation system between octaethylporphyrin (OEP) and *p*-substituted benzenes (Bzn–X), both chromophores of which are connected with a rigid and straight linkage of diacetylene (**1**: OEP–Bzn–X, Chart 1).[1] Based on their electronic spectra, an intramolecular charge-transfer (IaCT) interaction between these chromophores through the diacetylene linkage was studied and proved to be weakly induced in the derivative with electron-withdrawing X, like NO_2. Based on this finding, the electronic spectra of the conjugation system between OEP and 2-substituted 3-hexylthiophenes (**2**: OEP–HTh–X, Chart 1), which is a more sophisticated system, have been examined.[2] Since thiophene (Th) ring possesses the smaller resonance energy than Bzn ring,[3] Th should transfer the electronic effect of X more efficiently through a long-distant skeleton from one terminal site to another terminal OEP ring. In other words, the greater IaCT phenomena would be expected in the OEP–HTh–X system **2**. In fact, the IaCT absorption bands of **2** were observed more intensively and were proved to intensify regularly in order of the electron-withdrawing abilities of X. It was also shown that the transmission efficiency of the substituent effect of X to OEP in **2** enlarges nonlinearly with increasing Hammett substituent constant σ values, and yet, its transmission efficiency is much greater than that of the corresponding OEP–Bzn–X derivatives of **1**.

On the other hand, in order to develop new organic functional materials for supporting the present opto-electronics, a wide variety of well-defined and well-functioned conjugation systems based on heterocyclic nuclei, such as porphyrin and thiophene rings, have been demonstrated, by virtue of their high susceptibilities to optical and electronic stimulations.[4] In relation to the intense research of the opto-electronic devices, we have been studying the electronic properties of the 3,3′-dihexyl-2,2′-bithiophene (DHBTh) system, which is a dimer of HTh, through the comparative studies with the properties of its orientational isomers of various types. The reason for introducing HTh into our system is as follows. In designing organic functional materials, the material must be thermally and photochemically stable, have steady functions, and have easily accessible and controllable structures of the building blocks. A hexyl chain was incorporated into the main skeletons in consequence of optimization of the material processibility and the molecular density convenient for various optical devices, in terms of its chain length and bulkiness.[5] MM2 calculation clearly indicates that the π-electronic conjugation planarity of the fundamental DHBTh units increases in order of the orientation mode of two HTh rings in DHBTh: head-to-head (HH) < head-to-tail (HT) < tail-to-tail (TT).[5c] The orientation of DHBTh would bring about the respective molecular peculiarities, not only in the electrostatic properties but also in the chemical reactivities and mechanistic processes as a consequence (Chart 1).[6] In particular, from studies on the IaCT donor–acceptor DHBTh system, in relation to various molecular functionalities, such as non-linear optical (NLO) behaviors,[7] a structure–property relationship was experimentally observed between the greater third-order NLO response in the DHBTh derivative and the higher conjugation planarity.[8] More recently, an extended π-electronic conjugation system of DHBTh derivatives connected with OEP has been demonstrated to figure out features that are needed for opto-electronic devices.[9] OEP–DHBTh–OEP systems, connected with a diacetylene linkage, have unique electronic absorption bands in the region of 400–500 nm characteristic of OEP nucleus and the Soret band was split regularly into two main bands in response to the orientations of DHBTh. In addition, electrochemical experiments clearly showed that their electron-releasing abilities changed with respect to the π-electronic conjugation planarity of the DHBTh constituents.[10]

In our continuing investigations of the structure–property relationship of the DHBTh derivatives, isomeric pairs of the

Published on the web February 13, 2007; doi:10.1246/bcsj.80.371

R=C_6H_{13}, **a**: X=H, **b**: X=Br, **c**: X=CN, **d**: X=CHO, **e**: X=NO_2

1: OEP-Bzn-X **2:** OEP-HTh-X

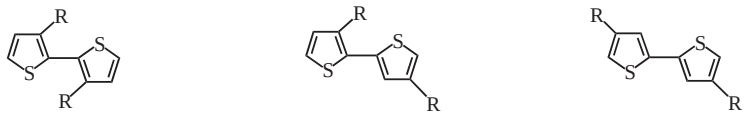

(HH)DHBTh (HT)DHBTh (TT)DHBTh

3: OEP-(HH)DHBTh-X **4:** OEP-(TT)DHBTh-X

Chart 1.

OEP–DHBTh–X system **3** and **4** were synthesized, in which the orientations of DHBTh are HH and TT modes with the lowest and highest π-electronic conjugation planarity, respectively (Chart 1). Their spectral properties were examined to determine the orientation effects of DHBTh and the substituent effects of X on the IaCT bands in this system. An aim of the subject in this study is to evaluate the substituent effect of X quantitatively on their absorption spectral properties and then to derive some structural requirements for enhancement of IaCT, based on the transmission efficiency of substituent effect in respective conjugation systems. Taking these results together with electrochemical experiments, the electronic properties of **3** and **4** were elucidated. While preparing the cyano (X = CN) derivatives **3c** and **4c**, a curious finding due to the orientation of DHBTh was also observed. In this paper, the syntheses and properties of **3** and **4** are described, in terms of orientation and substituent effects on their properties, in comparison to those of the related compounds **1** and **2**.

Results and Discussion

Syntheses of 1–4. Syntheses of the OEP–Bzn–X and OEP–HTh–X derivatives **1** and **2** were performed by the cross-coupling reactions of OEP terminal acetylene **5** and corresponding Bzn–X or HTh–X acetylenes (**6** or **7**) under the Eglinton conditions (Scheme 1).[1,2,11] Similarly, as summarized in Schemes 2–4, OEP–DHBTh–X derivatives **3** and **4** were synthesized by the reaction of **5** with corresponding DHBTh–X acetylenes **12** or **16**, respectively. DHBTh–X terminal acetylenes **12** and **16** were prepared from the respective bromo compounds (**9** and **15**: Br–DHBTh–X) with trimethylsilylacetylene (TMSA) under the Sonogashira conditions,[12] followed by alkaline hydrolysis. Among Br–DHBTh–X, the preparation of X = CN compound **9c** should be particularly noted. As is known for electrophilic substitution reactions on Th ring,[13] Br–DHBTh–NO_2 (**9e**) can be obtained directly by nitration

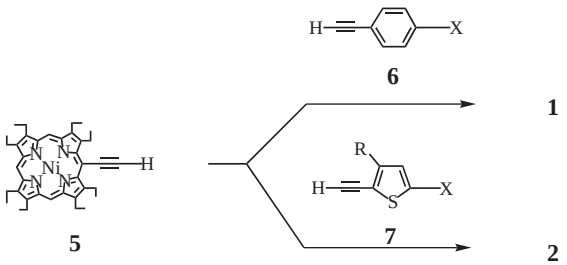

R=C_6H_{13}, **a**: X=H, **b**: X=Br, **c**: X=CN, **d**: X=CHO, **e**: X=NO_2

Scheme 1.

of Br–DHBTh–H (**9a**)[8,14] with nitric acid–acetic anhydride (HNO_3–Ac_2O) in good yield. Similarly, the selective transformation of Br–DHBTh–Br **9b** to Br–DHBTh–CHO **9d** occurred smoothly, by displacement of Br substituent with *n*-BuLi and *N*,*N*-dimethylformamide (DMF).[15] However, the transformation of one Br substituent of **9b** to the CN group by conventional methods, for example, with copper(I) cyanide (CuCN) in refluxing 1-methyl-2-pyrrolidinone (NMP), was not successful, resulting in a complex mixture of **9c** with a large quantity of **9b** and its dicyano product (^{1}H NMR and MS spectra). In addition, the mixture could not be separated completely, unlike a mixture of Br–HTh–Br, Br–HTh–CN, and CN–HTh–CN derivatives (see Experimental part). As well, under much milder conditions, the dibromo starting material **9b** was almost recovered, but its reproducibility was very poor. The electrophilic bromination of H–DHBTh–CN **10** with NBS in acidic media was also unsuccessful.[16] After several attempts, as outlined for the preparation of all Br–DHBTh–X derivatives **9a**–**9e** in Scheme 2, both **9c** and **15c** were successfully afforded by dehydration from the corresponding oximes **11** and **13** of aldehydes **9d** and **15d**.[17] In the course of transformation of X = CHO to X = CN via oximes, an orientation effect of DHBTh

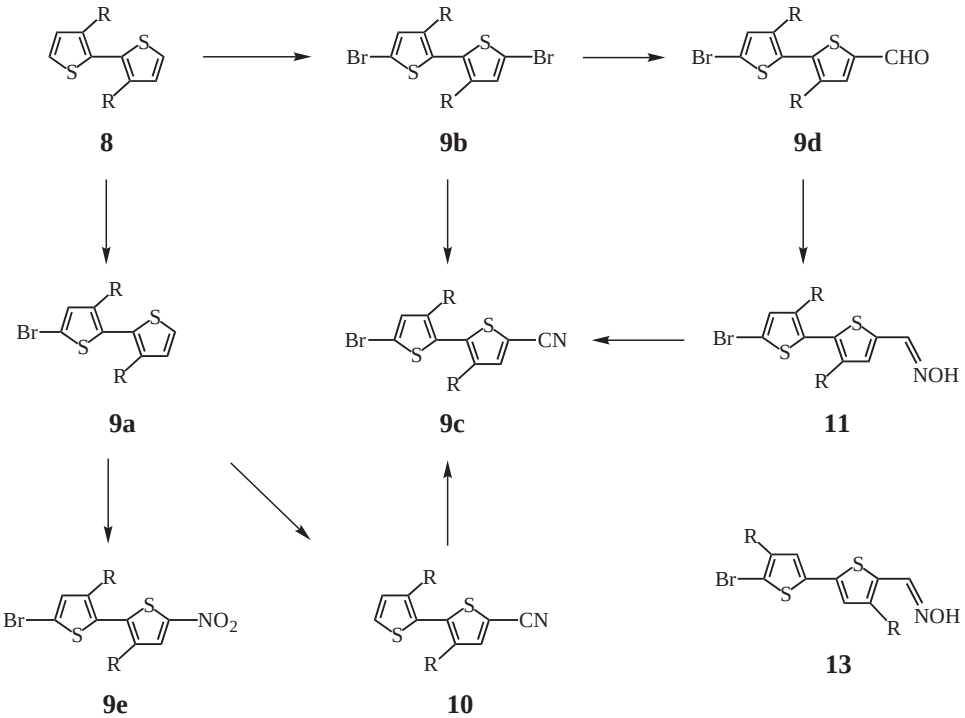

Scheme 2.

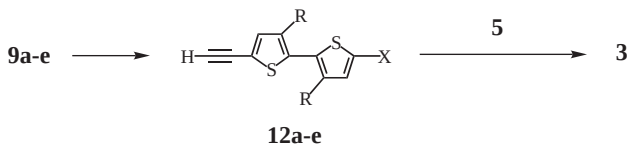

Scheme 3.

was observed (vide infra). The Br–DHBTh–X derivatives **9** and **15** thus obtained were readily converted with TMSA into the corresponding DHBTh–X terminal acetylenes **12** and **16** in good yields. Finally, oxidative couplings of the terminal acetylenes,[11] i.e., **5** with **12** or **16**, in the presence of copper(II) acetate [$Cu(OAc)_2$] afforded **3** and **4**, respectively, in moderate yields, together with homo-coupling dimeric products **17**–**21** (Chart 2). The structures of DHBTh derivatives of **1**–**4** were determined by MS, IR, and ^{1}H NMR spectra, as well as by elemental analyses.

Transformation of X = CHO to X = CN in the Br–DHBTh–X Derivatives. The CN derivatives **9c** and **15c** were prepared via oximes from the corresponding CHO derivatives **9d** and **15d**, respectively (Schemes 2 and 4). In the reaction of **9d** with hydroxylamine (NH_2OH), an 1:1 isomeric mixture **11** of syn-oxime ($R_f = 0.14$ based on $CHCl_3$) and anti-oxime ($R_f = 0.35$) was obtained. Mixture **11** could easily be separated by column chromatography on silica gel (SiO_2) into each product, and their isolated yields were almost identical to the ^{1}H NMR spectral yields. In ^{1}H NMR spectra, both the peak shapes and chemical shifts of syn- and anti-isomers are almost the same, except for a difference in the peak shape of their OH group. The peak due to OH proton of the syn-isomer appeared at around $\delta = 7.6$ ppm as a very sharp line, while that of the anti-isomer appeared at the same position as a very broad line. A similar phenomenon was observed in IR spectra, in which the peak for ν_{OH} of the syn-isomer (3277 cm^{-1} with less than 100 cm^{-1} half-width) was very sharp and for the anti-isomer ($\nu = 3500$–$2900\,cm^{-1}$) was very broad. Similarly, the TT isomer **15d** afforded a mixture of syn- and anti-oximes **13** (Scheme 2), and the isomers could be separated using a thin-layer chromatography ($R_f = 0.13$ for syn-isomer and $R_f = 0.33$ for anti-isomer, based on $CHCl_3$). The isomeric oximes **13**, however, were found extremely fragile in their respective forms in ordinary solvents. In fact, it was proved that any mixtures of oximes **13** in $CHCl_3$ spontaneously changed to the same equilibrium mixture between syn- and anti-isomers within a few minutes at room temperature (see Experimental part).

Such a spectral difference between HH and TT oximes **11** and **13** also appeared in the dehydration from them in both reactivity and yield. In the case of **11**, the syn-isomer reacted with the combined reagents of acetic anhydride and sodium

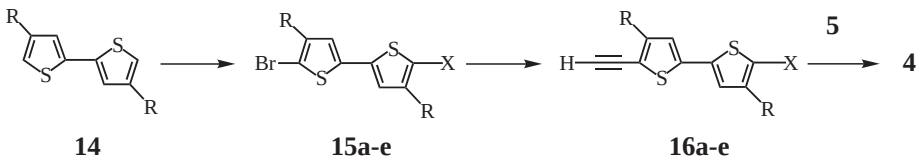

Scheme 4.

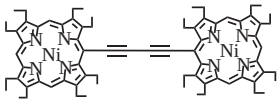

17

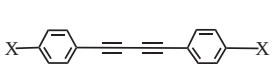

18

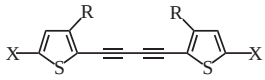

19

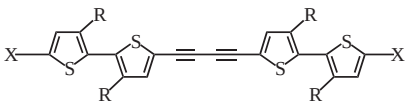

20

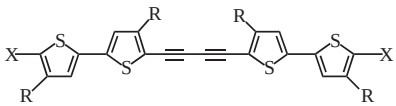

21

Chart 2.

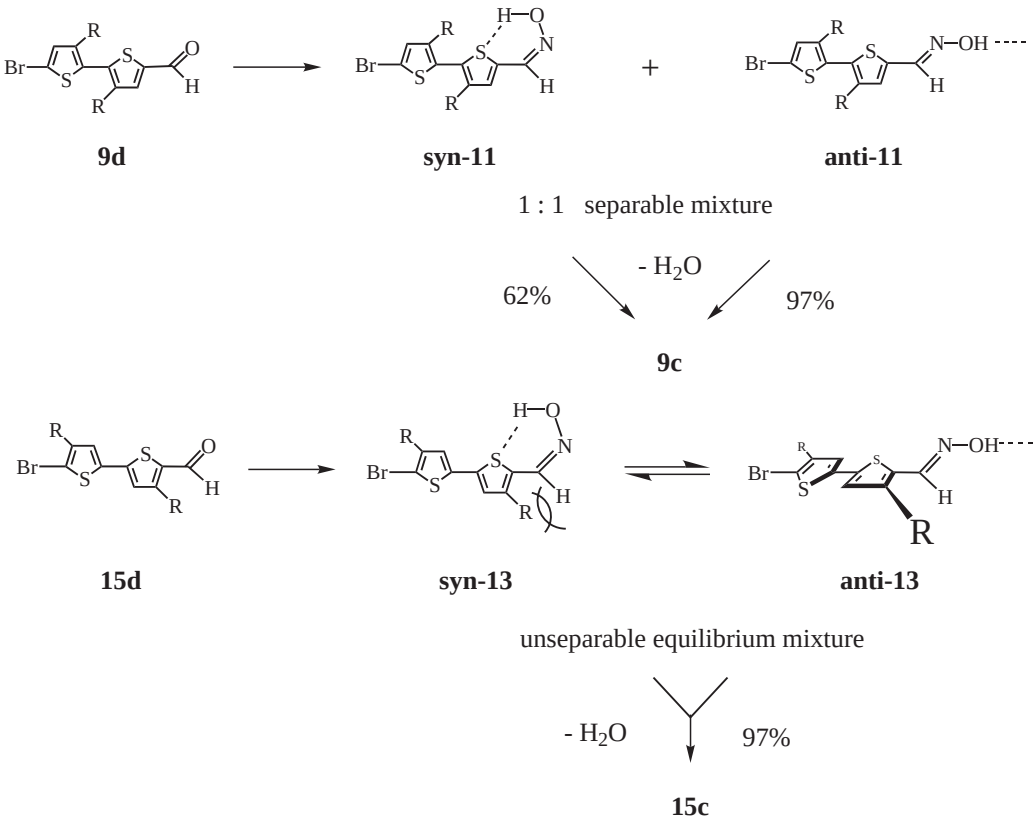

Scheme 5.

acetate (Ac_2O–AcONa) to form Br–DHBTh–CN **9c** in 62% yield,[17] while the anti-isomer reacted much faster under the same conditions to afford **9c** in 97% yield. On the other hand, the dehydration of the oxime mixture of **13** also proceeded very smoothly, similar to the anti-oxime of **11**, to produce the corresponding CN derivative **15c** almost quantitatively.

These results could be ascribed to the structural difference between oximes **11** and **13**. The syn-oxime produces additional stabilization energy through an intramolecular hydrogen bonding between OH group and sulfur atom of HTh ring, which should be greater than that produced into the anti-oxime through an intermolecular hydrogen bonding (Scheme 5). In other words, it is deducible that the intramolecular hydrogen bonding plays a crucial role in the isolation of the syn-oxime of **11** from the anti-isomer. On the other hand, in the case of syn-oxime **13**, such an intramolecular hydrogen-bonding interaction for its thermal stability is rather to force the molecule into a restricted geometry, where additional steric repulsion between C–H bond on the oxime moiety and hexyl substituent on the HTh ring arises to compete with the intramolecular

a: X=H, **b**: X=Br, **c**: X=CN, **d**: X=CHO, **e**: X=NO_2

1 **2**

3 **4**

22: Bzn-X **23:** Th-X

Chart 3.

hydrogen-bonding interaction. These antithetical interactions in the syn-oxime **13** cause the molecule to be much reactive. Instead, the anti-isomer would eliminate the sterical disadvantage by rotating the hydroxyimino group about a pinch bond to some degree, though the π-electronic conjugation for stabilization between C=N bond and Th ring is cut off as a consequence. Therefore, in the case of oximes **13**, it is concluded that the intramolecular hydrogen bonding of OH group with sulfur atom of HTh ring makes the free energy difference between syn- and anti-isomers less making it difficult to isolate each of them.

It should be noted that several molecular peculiarities due to the steric interaction of the hexyl group with additional substituents in the molecule have been curiously observed till now in the DHBTh derivatives of various types, especially in the DHBTh derivatives with TT orientation.[6,18] The phenomenon introduced above is exactly the one reflecting the orientation of the DHBTh constituent in the molecule (also see below).

^{1}H NMR Spectra. ^{1}H NMR spectra were very useful for making not only the structure determination of the molecules but also the orientation and substituent effects on the series of specific protons confirmed precisely, because of the rigid and simple structural system of the derivatives connected with the diacetylene linkage. Therefore, each proton could be easily assigned. All of the chemical shifts due to meso protons (meso-H) of the OEP ring in **1**–**4** were nearly the same ($\delta = 9.4 \pm 0.03$ ppm), clearly indicating that any substituents possess no ability enough to affect the ring current of OEP, apparently due to the long distance between them. On the other hand, series of Bzn- and Th-protons (Bzn–H and Th–H) near the substituents X exhibited their characteristic behaviors, depending on their individual circumstances, as is seen in the case of monosubstituted Bzn–X and Th–X derivatives **22** and **23** (Chart 3). It is well known that Hi series at the position next to X in **22** shifts toward the lower field from 7.25 ppm (**a**: X = H, in $CDCl_3$) regularly by the following magnitudes: 0.00 ppm for X = Br, 0.30 ppm for X = CN, 0.73 ppm for CHO, and 0.97 ppm for X = NO_2.[19] Similarly, Hk series at the 3-position in **23** shifts from 7.10 ppm (**a**: X = H, in $CDCl_3$) by the following magnitudes: −0.05 ppm for X = Br, 0.47 ppm for X = CN, 0.65 ppm for X = CHO ppm, and 0.82 ppm for X = NO_2.[20] It is shown that X = Br scarcely affects on the chemical shifts of both Hi and Hk, which is almost identical to X = H in magnetic affection. In other words, the substituent effects involving **22** and **23** substantially have the same trend, though the changes in the chemical shifts from the standard ones **22a** and **23a** are different in magnitude between Hi ($\Delta\delta = 0.00$–0.97 ppm) and Hk ($\Delta\delta = -0.05$–0.82 ppm) series. There was almost no change in the chemical shifts for Hh at the meta-position in **22** are almost unchanged. It is also interesting to note that among substituents X, only CN group affects the Th ring more strongly than the Bzn ring, resulting in nearly the same chemical shifts for Hi of **22c** and Hk of **23c**. These results should be ascribed not only to a structural difference between six-membered carbocyclic ring and five-membered heterocyclic ring, but also to a magnetic difference between ring currents of Bzn and Th nuclei.[21]

All of the chemical shifts for Th–H and Bzn–H in **1**–**4** were plotted against the substituents X, temporarily applying the changes in chemical shifts for Hi series in **22** or for Hk series in **23** as a measure of the substituent effects of X (Figs. 1 and 2). In the case of OEP–Bzn–X **1**, Ha series shifted in the region $\delta = 7.62$–7.77 ppm with changing X, while Hb series shifted in the region $\delta = 7.37$–8.26 ppm along an imaginary line involving Hi series. This result apparently indicates that Hb series adjacent to X are strongly affected, shifting toward lower fields on going from X = H to X = NO_2. The former Ha series are inherently much less affected by the substituents, similar to Hh series at the meta-position of **22**, simply reflecting the anisotropic effect of the diacetylene linkage to resonate at the relatively low fields in a very narrow region. As is generally known for Hi series in **22**, in addition to an electron-withdrawing effects of X on the ortho-position, an anisotropic effect of

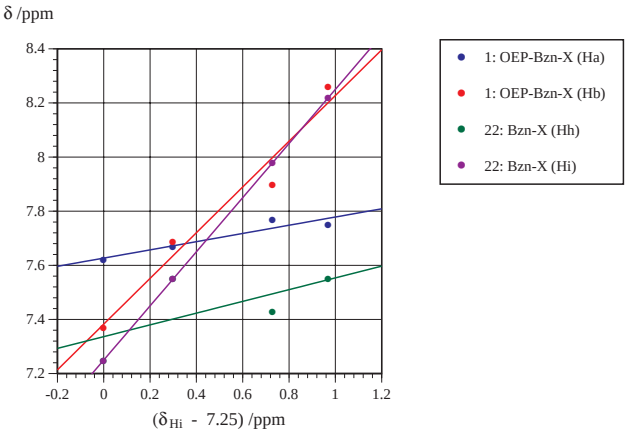

Fig. 1. Plots of chemical shifts of respective series of protons: **Ha** and **Hb** of **1** and **Hh** of **22**, against the shifting values of **Hi** series of **22**. 0.00 ppm for X = Br, 0.30 ppm for X = CN, 0.70 ppm for X = CHO, and 0.97 ppm for X = NO_2 were used as a measure of the substituent effects of X, based on 7.25 ppm of **Hi** of **22a**.[19]

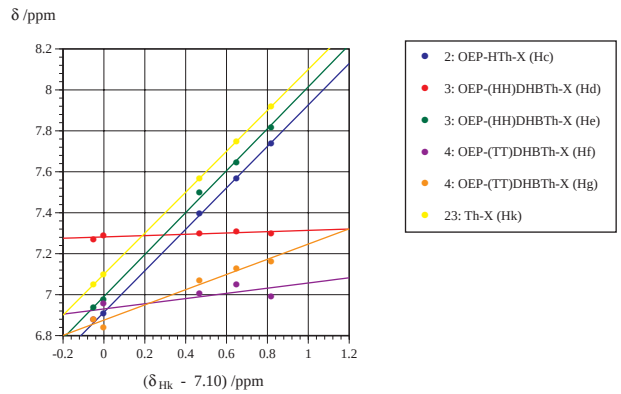

Fig. 2. Plots of chemical shifts of respective series of protons: **Hc**, **Hd**, **He**, **Hf**, and **Hg** of **2**, **3**, and **4**, against the shifting values of **Hk** series of **23**. −0.05 ppm for X = Br, 0.47 ppm for X = CN, 0.65 ppm for X = CHO, and 0.82 ppm for X = NO_2 were used as a measure for the substituent effects of X, based on 7.10 ppm of **Hi** of **23a**.[20]

the substituents carrying unsaturated bonds, such as X = CN, CHO, and NO_2, induces Hb series in **1** to change more drastically. The chemical shifts due to Ha and Hb in OEP–Bzn–CN **1c** were nearly the same, proving that the magnetic influences on Bzn–H are almost comparable between the CN substituent and the diacetylene-group connected OEP constituent.

In the case of OEP–HTh–X **2**, the chemical shift changes for Hc series were considerably correlated with those for Hk series in **23**, apparently showing that the substituent effect on Th ring of **23** holds purely in parallel on HTh ring of **2**. A series of Hc, however, all resonate at the higher fields (δ = 6.91–7.74 ppm), as compared with the corresponding Hk series. This result might be ascribed to a reduction in the HTh ring current of **2** due to the multiple substituents on it, rather than to a combined shielding effect of the diacetylene linkage as an electron-withdrawing substituent and the hexyl group as an electron-donating substituent on Hc series (vide infra).

The trend in chemical shift changes for Th–H series in **23** was similarly and explicitly observed for that of the OEP–DHBTh–X systems **3** and **4** (Fig. 2). In the respective Th–H series attached on HTh ring linked with the diacetylene, Hd series appeared in the region δ = 7.27–7.31 ppm for HH isomer **3** and Hf series in the region δ = 6.88–7.05 ppm for TT isomer **4**, indicating that each Th–H series exists in the very similar magnetic circumstance and are substantially free from affections of X. In the case of Th–H series attached to the HTh ring linked with the substituents X, the chemical shifts for Hg series in **4** are comparable to those for Hj series in **23**, and thus, the two proton series are similar to each other, with the changes in the chemical shift in the narrow region δ = 6.84–7.16 ppm. On the other hand, as expected, substituent effects were clearly observed for only He series in **3**, with the changes in the chemical shift in the region δ = 6.98–7.82 ppm, with a high similarity to the behavior of Hk series. It is also notable that the chemical shifts for He series are all observed in an in-between region of the Hc and Hk series. Since the Th ring is generally regarded as an electron-donative nucleus,[22] He series should appear at higher fields than the corresponding Hc series, if shielding effect was only considered. Therefore, this reversed result could be ascribed to that the 2-substituted HTh ring in **3** recovers its ring current with a greater magnitude consequently, as compared with that in **2**, because the electron-withdrawing diacetylene linkage is located far away from the 2-substituted HTh ring moiety.

Although a linear correlation between substituents and the changes in chemical shifts for Bzn–H and Th–H was observed, it seemed parameters like, Hammett substituent constant σ values, could not be applied in these systems. As is generally the case, a hard correlation between substituent effects on Bzn–H and Th–H adjacent to X and certain σ values involves additional factors, such as steric and electronic interactions between X and peripheral substituents on the respective rings. With such a restricted structural situation around the ortho-position of X, the substituent effect would not appear in all the derivatives with the same efficiency. Thus, the substituent effects in **1**–**4** were relatively compared with those in **22** and **23**, based on the chemical shift changes for Hi or Hk series as the imaginary substituent constant σ values for X. As given in Equations 1–4, among Bzn–H and Th–H, Hb, Hc, He, and Hg series possess the fairly high similarity in substituent effect to Hi or Hk series with correlation factors R of greater than 0.96. The substituent effect of X transfers comparably onto these four series of **1**–**4** in the very similar mechanism to that in the standard compound **22** or **23**, with various efficiencies depending on their individual circumstances. The substituent effect on Hb series in **1** is described by that of Hi series with 84% efficiency (Eq. 1). In particular, it is evident in a quantitative sense that both Hc and He series exist in the same magnetic circumstance as Hk series (Eqs. 2 and 3), as could also be deduced from Fig. 2.

$$\delta = 0.84\sigma + 7.38 \ (R = 0.961, \text{ for the Hb series}) \quad (1)$$

$$\delta = 1.01\sigma + 6.91 \ (R = 1.000, \text{ for the Hc series}) \quad (2)$$

$$\delta = 1.02\sigma + 6.91 \ (R = 0.998, \text{ for the He series}) \quad (3)$$

$$\delta = 0.37\sigma + 6.88 \ (R = 0.968, \text{ for the Hg series}) \quad (4)$$

Although the changes in the chemical shift for Hj series at

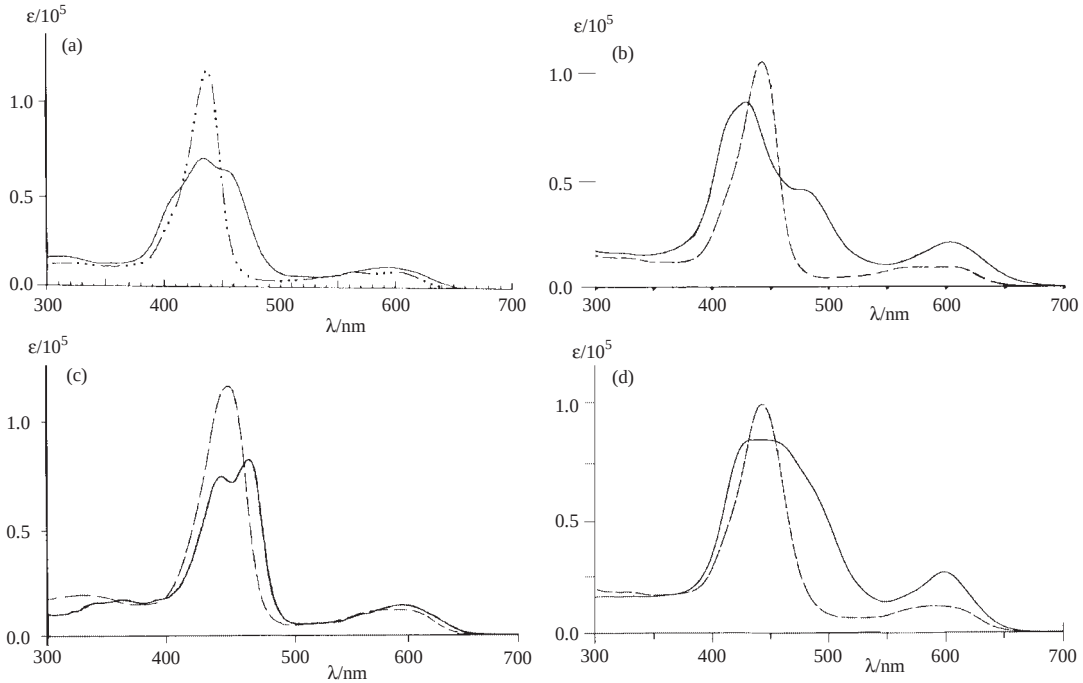

Fig. 3. Electronic absorption spectra for pairs of the X = H and X = NO_2 derivatives in respective systems ($CHCl_3$, 25 °C). (a) is for **1a** (broken line) and **1e** (solid line), (b) is for **2a** (broken line) and **2e** (solid line), (c) is for **3a** (broken line) and **4a** (solid line), and (d) is for **3e** (broken line) and **4e** (solid line).

the 4-position in **23** show no regular trend upon changing X: −0.27 ppm for X = Br, 0.00 ppm for X = CN, 0.10 ppm for X = CHO, and −0.03 ppm for X = NO_2,[20] while Hg series in **4** behaved similarity to Hk series (Eq. 4). The reason for such a high similarity in chemical shift changes between Hg and Hk series is not understood at present. The substituent effect on Hg series, however, is fairly small (37% transmission efficiency based on Hk series), probably due to their distance from X.

Electronic Absorption Spectra. Electronic absorption spectral measurements were performed in $CHCl_3$ at room temperature, unless otherwise stated. Selected spectra of respective pairs of derivatives with substituents **a**: X = H and **e**: X = NO_2 in **1**–**4** are shown in Fig. 3. Among them, Figures 3c and 3d show a pair of **3a** and **4a** and a pair of **3e** and **4e**, respectively, for convenience sake.

The X = NO_2 derivatives **1e**, **2e**, and **4e** exhibit much different spectra from the corresponding X = H derivatives **1a**, **2a**, and **4a**, affording much broad absorption curves, distinct from the case of a pair of **3a** and **3e**. Almost symmetrical Soret bands ($\pi \rightarrow \pi^*$ transitions) of **1a** and **2a** showed a tendency to split into two or three main bands, when X = H is replaced with the more electron-withdrawing substituents toward X = NO_2, respectively, with a reduction in their intensities. In the case of **3**, the Soret bands were nearly the same between **3a** and **3e** in both absorption maximum and shape, appearing in single absorption curves (Figs. 3c and 3d). On the other hand, the Soret band for **4a** is split into two clear bands,[23] while the Soret band for **4e** is almost one broad band with a slightly distorted shape in $CHCl_3$. It was also shown that the spectra of X = Br derivatives are similar to those of X = H derivatives for each series and that the other X = CN and CHO derivatives had spectra in-between those of the X = H and NO_2 derivatives, as is seen

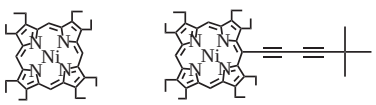

24 **25**

Chart 4.

in their ^{1}H NMR spectra. With respect to Q bands ($n \rightarrow \pi^*$ transitions), derivatives **1a** and **2a** exhibited much broader bands with less intensity, as compared to derivatives **1e** and **2e**. In the case of **3** and **4**, Q bands of the (TT)DHBTh derivatives are slightly sharper and more intense than those of the corresponding HH isomers, with longer tailing.

From a previous study, the diacetylene linkage efficiently shifts the maximum of Soret band of OEP (**24**; λ_{max} = 393 nm in $CHCl_3$)[24] by 35 nm without altering the electronic structure, suggesting that the diacetylene linkage in **25** (λ_{max} = 428 nm)[1,25] is an inductive substituent rather than part of the π-electronic conjugation (Chart 4). Similarly, the connection of the diacetylene-group OEP derivative **25** to other chromophores, such as Bzn and HTh moieties, at the terminal position caused further bathochromism in the Soret band maximum, which shifted by another 7 nm for **1a** and 16 nm for **2a**. This result shows that the HTh ring system electronically interacts with OEP through the diacetylene linkage more intensively. The terminal HTh constituents in **3**, however, exhibited no longer affection on the OEP ring, distinct from those in **4**, clearly indicating that the high π-electronic conjugation planarity of DHBTh in the molecular system is very important for electronic communication between such far-distant separated chromophores (vide infra).

Table 1. Solvent Dependent Absorption Maxima (λ/nm) Due to IaCT Bands of the Nitro Derivatives of **1**–**4**

OEP derivatives	Hexane	Acetonitrile	ΔE/kcal mol^{-1}
1e	459	445	1.92
2e	483	453	3.85
3e	442	440	0.29
4e	488	468	2.45

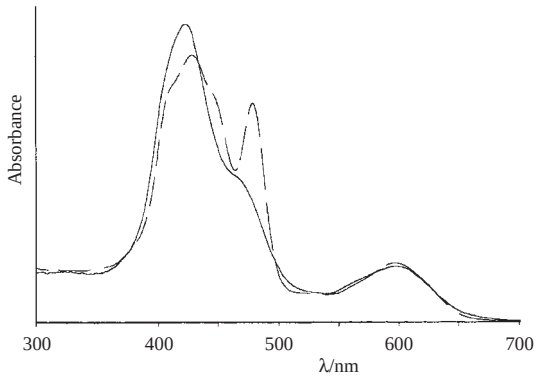

Fig. 4. Electronic absorption spectra of **2e** in hexane (broken line) and in acetonitrile (solid line).

It should be noted that the orientation of DHBTh also plays a critical role in the external conjugation with the 18 π-electronic conjugation ring system of OEP through the diacetylene linkage, which splits the Soret band into two or three bands.[26] The splitting in the Soret bands were found to be affected by both the substituents and solvent polarities, i.e., a larger bathochromic shift was observed with a stronger electron-withdrawing X and with less polar solvents.[1,2,8,23,27] Accordingly, these bands were assigned as IaCT bands, indicating that the OEP derivatives in these systems are more polarized in the ground state.[26] The IaCT bands of **1e**–**4e** in hexane (non-polar) and acetonitrile (polar) solvents are summarized in Table 1, and the spectra for **2e** are shown in Fig. 4. Since no particular spectral changes were observed upon changing not only substituents but also solvent polarities for all the derivatives **3**, which is similar to **24** and **25**, the substituents X have negligible affect on **3**. Therefore, it could be concluded that the electronic structures of OEP nuclei in these diacetylene-group connected conjugation systems are sensitive to the solvent polarity in order of **2e** > **4e** > **1e** ≫ **3e**.

According to Rao, the maxima due to the IaCT bands in the donor–acceptor Bzn derivatives, such as *p*-substituted anilines and anisoles, are well known to correlate linearly with Hammett substituent constant σ values.[28] However, similar to the ^{1}H NMR spectral study, no adequate set of σ values have been reported to the best of our knowledge until now, which can be used for the systems **1**, **2**, and **4**. Thus, simply applying Rao's equation ($\lambda = \lambda_0 + \rho\sigma$) to IaCT bands of **1**, imaginary σ values for X were estimated from their Soret band maxima based on **1a** ($\lambda_{max} = 435$ nm) in order to establish a linear correlation between them, affording $\sigma = 0.00$ for X = H (Br), 0.25 for X = CN, 0.50 for X = CHO, and 1.00 for X = NO_2 with $\rho = 20.0$; the absorption maximum of **1a** is completely the same as that of **1b** (Eq. 5). In view of the same skeletons between **1**–**4**, their IaCT bands were plotted against the estimated σ values (Fig. 5), and curve fitting of λ-σ correlations for **2** and **4** led to the fairly high linear relationships between them (Eqs. 6 and 7).

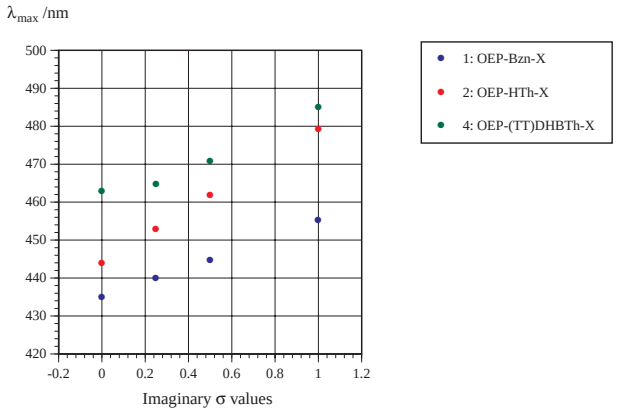

Fig. 5. Plots of IaCT band maxima of **2** and **4**, based on IaCT bands of **1** ($CHCl_3$, 25 °C). For linear correlation between IaCT band and substituent effect, σ values for X of **1** were defined by using $\lambda_{max} = 435$ nm of **1a** as 0.00 for X = H (Br), 0.25 for X = CN, 0.50 for X = CHO, and 1.00 for X = NO_2 with $\rho = 20.0$ ($R = 1.000$).

$$\lambda = 435 + 20.0\sigma \ (R = 1.000, \text{ for series } \mathbf{1}) \quad (5)$$

$$\lambda = 444 + 35.0\sigma \ (R = 0.999, \text{ for series } \mathbf{2}) \quad (6)$$

$$\lambda = 461 + 22.9\sigma \ (R = 0.965, \text{ for series } \mathbf{4}) \quad (7)$$

Based on these results, the substituent effect in **2** transmits to the terminal OEP electronic system through the diacetylene linkage mechanistically in the same manner to the OEP electronic system as in **1**. Yet, the transmission efficiency of the substituent effect in **2** is 1.75 (35.0/20.0) times greater in the λ value (1.65 times greater in energy value) than that in **1**. This result could be attributed to the cyclic 6π-electron conjugation system of both Bzn and Th nuclei but to the smaller resonance energy of the Th ring, which is eventually almost comparable to the difference in an aromaticity index, estimated as ISE scale, between the Bzn (58.20 kcal mol^{-1}) and Th (32.54 kcal mol^{-1}) rings.[29] On the other hand, the linear correlation factor R for the derivatives of **4** was slightly small (0.965), and a turning point in the substituent effect was clearly observed at X = CN. In the conjugation system of **4**, two types of electronic interactions of OEP with the (TT)DHBTh constituent vs with the X substituents might affect their IaCT bands concurrently. The above result suggests that the interaction of OEP with X is dominant over the interaction with the DHBTh constituent, in the derivatives that have X with σ values greater than 0.25 (also see below). It is also noted that the transmission efficiency of the substituent effect on the IaCT bands is still almost comparable in energy value range between **1** (2.9 kcal mol^{-1} from X = H to X = NO_2) and **4** (2.8 kcal mol^{-1}), in spite of the longer distance between OEP and X in **4**. This result apparently indicates the greater susceptibility of Th ring to outside stimulations, such as X and solvent effects. Furthermore, it was found that the substituent effect (X = H/NO_2) on IaCT bands is comparable to the solvent ef-

Table 2. Half-Wave Oxidation Potentials (/mV)[a] of Substituted OEP Derivatives **1**–**4** and Related Compounds **24** and **25**

OEP derivatives	$E_1^{1/2}$ / $E_2^{1/2}$				
	a: X = H	**b**: X = Br	**c**: X = CN	**d**: X = CHO	**e**: X = NO_2
1	915	915	940	975	1010
	1280	1285	1310	1350	1390
2	900	910	930	940	950
	1260	1280	1250	1290	1300
3	910	915	920	930	920
	1280	1210	1260	1300	1270
4	870	880	980	910	910
	1240	1200	1360	1260	1190
24	860				
	1320				
25	910				
	1280				

a) Oxidation potentials were measured by cyclic voltammetry in CH_2Cl_2 containing *n*-Bu_4NClO_4. GC (working E), Pt (counter E), and SCE (reference E). Scan rate; 120 mV s^{-1}.[31]

fect (hexane/acetonitrile) in terms of energy value range, in these diacetylene-group connected OEP derivatives.

Oxidation Potentials. Porphyrins are highly susceptible to optical and electrochemical stimulations to produce corresponding radical cations by releasing one electron, with which versatile sensitization functions are driven in various living bodies including photo-synthetic reaction center.[30] Thus, in this study, the oxidation potentials of the OEP derivatives in **1**–**4** were measured by cyclic voltammetry for estimation of the substituent effect on their electron-releasing ability in dichloromethane (CH_2Cl_2) (Table 2).[31] All of the OEP derivatives including **24** and **25** exhibited the reversible redox waves in the potential region between 860 and 1390 mV vs SCE, with two one-electron releasing processes toward the corresponding dicationic species. Based on the result (E_1 = 910 mV) of **25**, the diacetylene linkage proves to heighten the first oxidation potential (E_1 = 860 mV) of **24**, indicating the electron-withdrawing ability of the diacetylene linkage to lower the HOMO of **24**. The HOMO of OEP is a non-bonding level involving four peripheral N atoms of OEP.[32] The diacetylene linkage, however, can be rather regarded as an inductive substituent and, thus, lowers the LUMO of OEP more efficiently, since not only Soret but also Q bands of **25** appeared at the much longer wavelengths than the respective bands of **24**. Similarly, the E_1 values of **1a** and **2a** are almost equal to that of **25**, indicating that the π-electronic conjugation interaction between OEP and Bzn or HTh nuclei through the diacetylene linkage affects mostly the LUMO of **24**, but not its HOMO so much. There is a relatively large difference in the E_1 values of **3a** and **4a**, proving that the terminal HTh ring of the (TT)DHBTh constituent in **4** participates efficiently in the π-electronic conjugation interaction with OEP to elevate its HOMO. In this respect, the terminal HTh ring of the (HH)DHBTh constituent in **3** is just regarded as a sterical substituent, due to the highly distorted conjugation plane of DHBTh, showing that the effect of (HH)DHBTh on the HOMO is almost comparable to a *t*-butyl group.

Introduction of X into the OEP–Bzn–H and OEP–HTh–H systems heightens their oxidation E_1 values regularly, and thus, lowers their electron-releasing abilities with an increase in the electron-withdrawing properties of X. It is also noted that the transmission efficiency of the substituent effect on the HOMO is greater in the Bzn system (ΔE_1 = 95 mV from X = H to X = NO_2) than in the HTh system (ΔE_1 = 50 mV). Taking their electronic spectral results into consideration, this fact reversely indicates that the substituent effect on the LUMO is more prominent in the system of **2** consequently. As expected, the OEP–(HH)DHBTh–X system **3** exhibited almost the same E_1 values in such a narrow region of 910–920 mV for each X derivatives, showing that neither conjugation interaction effect nor substituent effect transfer to the OEP ring because the (HH)DHBTh constituent is distorted, which supports the results from the electronic spectra. On the other hand, the OEP–(TT)DHBTh–X system **4** showed a peculiar trend in the substituent effect on their HOMO, different from the systems **1** and **2**. Because of the highly conjugated planarity of (TT)DHBTh, the E_1 values of **4** were expected to heighten regularly with an increase in the electron-withdrawing abilities of X. In fact, the E_1 values of the first three derivatives **4a**, **4b**, and **4c** increased in order. However, the E_1 values of the rest derivatives **4d** and **4e** lowered to be almost equal to those of the X = H derivatives in the other systems. It is also noted that only in the case of **4**, the X = CHO and NO_2 derivatives possess higher electron-releasing abilities than the X = CN derivative. The difference in the substituent effect on the HOMO in **4** can be explained by the fact that an sp^2-atom containing X, such as CHO and NO_2, can not avoid the steric repulsion with the nearby bulky hexyl group on the terminal HTh ring. Thus, certain substituents X are distorted from the conjugation plane with HTh, resulting in a resonance interdiction between them more or less. Up to now, curious phenomena due to the steric repulsion of this type have been observed occasionally for the TT isomer of the DHBTh derivatives in terms of electron-transfer processes[33] and conformational changes,[6,18] as well as the dehydration reactivities from isomeric DHBTh oximes (vide ante).

Conclusion

According to the synthetic procedures for the OEP–Bzn–X derivatives **1**, series of OEP–HTh–X and OEP–DHBTh–X derivatives **2**, **3**, and **4** were successfully synthesized, utilizing oxidative couplings of the corresponding terminal acetylenes. In the course of synthetic study for OEP–DHBTh–CN **3c** and **4c** via oximes **11** and **13**, the hydroxyimino moiety was found to participate not only in an intramolecular hydrogen-bonding interaction with the sulfur atom of HTh ring but also in a sterically repulsive interaction with the hexyl group. This structural situation in antithetical interactions results in a characteristic difference in their stability and reactivity between syn- and anti-oximes. Substituent effects appear in the structural and spectral properties in relation to the electron-withdrawing abilities of X. The substituent effect was clearly observed in ^{1}H NMR spectra of the three series of Hb, Hc, and He, which is comparable to the corresponding series of Hi and Hk in **22** and **23**. Unexpectedly, the chemical shifts for Hg in **4** also changed linearly with the electron-withdrawing abilities of X, in contrast to those for Hj at the 4-position in **23**. In particular, the electronic absorption spectra were affected intensively not only by the substituent effect but also by the orientation of DHBTh. Using estimated σ values based on the IaCT bands in **1**, the maxima of IaCT bands in **2** proved to change regularly and exactly in the same mechanism as those in **1**. The (HH)DHBTh system **3** exhibited no particular relationship between X and their IaCT band maxima, while the maxima for the (TT)DHBTh system **4** changed regularly similar to those in **1**. These facts clearly show that the substituent effect can be efficiently transmitted to the electronic properties of OEP by increasing the molecular planarity even in such a long-distant conjugation system. In addition, it is concluded that the transmission efficiencies of substituent effect on both ^{1}H NMR and electronic spectra were greater in the HTh and DHBTh derivatives than in the corresponding Bzn derivatives, indicating that the smaller resonance energy of the Th ring makes it easier to be affected by the outside stimulations as well. The combined analysis of the absorption spectra with the electrochemical experiments revealed that the electron-withdrawing substituent effect appears mostly on the LUMO of OEP more intensively than on its HOMO, though both HOMO and LUMO undoubtedly lower their energy levels. Several trials for linear correlation of substituent constant σ values with the first oxidation potential E_1 value, as a measure of electron-releasing ability from the HOMO, met without success, but the trends in substituent effect on E_1 values were uniquely observed in the present series of OEP derivatives. Among them, both **1** and **2** decreased their electron-releasing abilities in order with the electron-withdrawing properties of X. And, the changes in the E_1 value between the X = H and X = NO_2 derivatives conclude that the substituent effect is transmitted to the HOMO with a greater efficiency in the Bzn system **1** and to the LUMO with a greater efficiency in the HTh system **2**. In the case of **3**, a trend in substituent effect on E_1 values was not particularly observed. Although the E_1 values for the derivatives of **4** were expected to increase in order of the electron-withdrawing abilities of X due to the high conjugation planarity of (TT)DHBTh, no regular trend in substituent effect was observed. This suggests a resonance interdiction between X with HTh ring arising from steric repulsion with the hexyl group. In order to verify the irregular trend in the substituent effect in **4**, further investigations are under way with a new series of long-distant conjugation derivatives, OEP–(TH)DHBTh–X (**26**, Chart 5).[34]

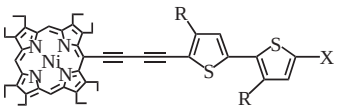

26: OEP-(TH)DHBTh-X

Chart 5.

Experimental

Melting points were determined on a hot-stage apparatus and are uncorrected. IR spectra were measured on a Jasco FT/IR 7300 spectrophotometer as KBr disk or neat sample; only significant absorptions are reported in ν values (cm^{-1}). EI and FAB mass spectra were recorded with a JEOL JMS-700 spectrometer. ^{1}H NMR spectra were measured in $CDCl_3$ solution at 25 °C on a JEOL JMN-ECP 600 (600 MHz) spectrometer and were recorded in δ value (ppm) with TMS as an internal standard. The coupling constants (J) are given in Hz. Electronic absorption spectra were measured in $CHCl_3$ solution on a Shimadzu UV-2200A spectrophotometer and were recorded in λ_{max} values (nm, sh = shoulder) and molar extinction coefficients (ε), unless otherwise stated. CV was performed on a BAS CV-27 potentiometer in CH_2Cl_2 solution in the presence of n-Bu_4NClO_4 at a scan rate of 120 mV s^{-1}.[31] SiO_2 (Fujisilysia BW 820MH or BW 127ZH) and aluminum oxide (Al_2O_3, CAMAG 504-C-1) were used for column chromatography. THF was distilled over calcium hydride and then over sodium diphenylketyl under argon (Ar) atmosphere before use. The reactions were followed by TLC aluminum sheets precoated with Merck SiO_2 F_{254} or with Merck Al_2O_3 GF_{254}. Organic extracts were dried over anhydrous sodium sulfate or magnesium sulfate prior to removal of the solvents.

2-Bromo-5-cyano-3-hexylthiophene. Method A (reaction with CuCN); a solution of 2,5-dibromo-3-hexylthiophene[14] (103 mg, 0.316 mmol) and CuCN (28.4 mg, 0.317 mmol) in NMP (3.0 cm^3) was stirred at 120–125 °C over 30 h. The reaction mixture was poured into 25% ammonia aqueous solution and was extracted with $CHCl_3$. The extracts were washed with brine and then dried. The residue obtained after removal of the solvent was chromatographed on SiO_2 (1.7 × 80 cm) with hexane–$CHCl_3$ (4:1) to afford 5-bromo-2-cyano-3-hexylthiophene (8.6 mg, 10%), 2-bromo-5-cyano-3-hexylthiophene (12 mg, 14%), and 2,5-dicyano-3-hexylthiophene (6.9 mg, 10%) in order, together with 2,5-dibromo-3-hexylthiophene (44 mg). **5-Bromo-2-cyano-3-hexylthiophene**: Yellow oil. MS; m/z 271, 273 (M^+, $M^+ + 2$, based on ^{79}Br) for $C_{11}H_{14}BrNS$. IR; 2955, 2930, and 2860 (CH), 2220 (CN). ^{1}H NMR; 6.95 (1H, s, Th–H), 2.74 (2H, t, J = 8 Hz, CH_2-$(CH_2)_4CH_3$), 1.70–1.20 (8H, m, $CH_2(CH_2)_4CH_3$), 0.89 (3H, t, J = 7 Hz, CH_3). UV–vis; 265 (12000). Found: C, 48.44; H, 5.33; N, 5.10%. Calcd for $C_{11}H_{14}BrNS$: C, 48.52; H, 5.18; N, 5.15%. **2-Bromo-5-cyano-3-hexylthiophene**: Yellow oil. MS; m/z 271, 273 (M^+, $M^+ + 2$, based on ^{79}Br) for $C_{11}H_{14}BrNS$. IR; 2955, 2930, and 2860 (CH), 2220 (CN). ^{1}H NMR; 7.31 (1H, s, Th–H), 2.80 (2H, t, J = 8 Hz, $CH_2(CH_2)_4CH_3$), 1.70–1.25 (8H, m, CH_2-$(CH_2)_4CH_3$), 0.89 (3H, t, J = 7 Hz, CH_3). UV–vis; 248 (7800),

256 (7700), 282 (10500). Found: C, 48.36; H, 5.22; N, 4.97%. Calcd for $C_{11}H_{14}BrNS$: C, 48.52; H, 5.18; N, 5.15%. **2,5-Dicyano-3-hexylthiophene**:[14a] MS; m/z 219 ($M^+ + 1$) for $C_{12}H_{14}N_2S$. IR; 2950, 2925, and 2860 (CH), 2225 (CN). ^{1}H NMR; 7.46 (1H, s, Th–H), 2.80 (2H, t, $J = 8$ Hz, $CH_2(CH_2)_4CH_3$), 1.70–1.25 (8H, m, $CH_2(CH_2)_4CH_3$), 0.89 (3H, t, $J = 7$ Hz, CH_3).

Method B (transformation via oxime); a solution of 2-bromo-5-formyl-3-hexylthiophene (2 g, 7.27 mmol) and hydroxylamine hydrochloride ($NH_2OH \cdot HCl$, 645 mg, 9.28 mmol) in pyridine–ethanol (Py–EtOH; 20 cm^3, 1:1 v/v) was stirred under reflux over 12 h. The mixture was concentrated under reduced pressure, admixed with water and extracted with $CHCl_3$. The extracts were shaken with dil. HCl, washed with brine and then dried. The residue obtained after removal of the solvent was recrystallized from $CHCl_3$–EtOH to afford the oxime (2.04 g, 97%) as pale yellow microcrystallines. The product should consist of syn- and anti-oximes, but its equilibrium ratio was hard to be analyzed. Thus, the characterization of the product was determined as an equilibrium mixture (also see below). Mp; 38–42 °C. MS; m/z 290, 292 ($M^+ + 1$, $M^+ + 3$, based on ^{79}Br) for $C_{11}H_{16}BrNOS$. IR; 3066 (br, OH), 2952, 2926, and 2856 (CH), 1638 (CNO), 1462 (NO). ^{1}H NMR; 8.13 (1H, s, HCNO), 7.59 (1H, s, OH), 6.88 (1H, s, Th–H), 2.57 (2H, t, $J = 8$ Hz, $CH_2(CH_2)_4CH_3$), 1.65–1.20 (8H, m, $CH_2(CH_2)_4CH_3$), 0.89 (3H, t, $J = 7$ Hz, CH_3). UV–vis; 262 (8840), 273 (9860, sh), 295 (15110). Found: C, 45.28; H, 5.77; N, 4.65%. Calcd for $C_{11}H_{16}BrNOS$: C, 45.51; H, 5.56; N, 4.83%. The oxime (1.90 g, 6.55 mmol) thus obtained was admixed with sodium acetate (20.3 mg, 0.25 mmol) in acetic anhydride (Ac_2O; 10 cm^3) and was stirred under reflux over 3 h. The reaction mixture was poured into dil. NaOH aq. and was extracted with $CHCl_3$. The extracts were washed with brine and then dried. The residue was purified in a similar way to Method A to afford 2-bromo-5-cyano-3-hexylthiophene (1.46 g, 82%).

2-Bromo-5-formyl-3-hexylthiophene. To a solution of 2,5-dibromo-3-hexylthiophene[14] (2.5 g, 7.67 mmol) in THF (25 cm^3) was added *n*-BuLi (1.6 M solution in hexane, 4.8 cm^3, 7.68 mmol) at −78 °C over 15 min. After stirring for additional 20 min, DMF (3.0 cm^3, 38.8 mmol) was added dropwise at −78 °C. The reaction mixture was gradually warmed up to room temperature and then poured into water and extracted with $CHCl_3$, successively. The residue obtained after removal of the solvent was chromatographed on SiO_2 (4.1 × 16 cm) with hexane to afford 2-bromo-5-formyl-3-hexylthiophene (1.61 g, 76%) as pale yellow oil, together with 2-bromo-3-hexylthiophene[14] (128 mg, 7%). **2-Bromo-5-formyl-3-hexylthiophene**: MS; m/z 275, 277 (M^+, $M^+ + 2$, based on ^{79}Br) for $C_{11}H_{15}BrOS$. IR; 2955, 2978, and 2857 (CH), 1672 (CO). ^{1}H NMR; 9.76 (1H, s, CHO), 7.46 (1H, s, Th–H), 2.60 (2H, t, $J = 8$ Hz, $CH_2(CH_2)_4CH_3$), 1.65–1.20 (8H, m, $CH_2(CH_2)_4CH_3$), 0.90 (3H, t, $J = 7$ Hz, CH_3). UV–vis; 271 (9300), 309 (11700). Found: C, 48.06; H, 5.62%. Calcd for $C_{11}H_{15}BrOS$: C, 47.99; H, 5.49%.

2-Bromo-3-hexyl-5-nitrothiophene. To a solution of 2-bromo-3-hexylthiophene (1.0 g, 4.05 mmol) in Ac_2O–THF (6 cm^3, 2:1 v/v) was added a mixture of HNO_3 (60% solution, 0.93 cm^3, 12.2 mmol) and Ac_2O (3 cm^3) at −40 °C over 15 min under Ar atmosphere, and the mixture was kept standing at 0 °C for 12 h. A solution of potassium hydroxide (KOH; 2 M solution in H_2O, 50 cm^3) was added to the reaction mixture at 0 °C, and then after 30 min stirring the mixture was extracted with $CHCl_3$. The extracts were washed with brine and dried. The residue obtained after removal of the solvent was chromatographed on SiO_2 (3.2 × 8 cm) with hexane–$CHCl_3$ to afford 2-bromo-3-hexyl-5-nitrothiophene (489 mg, 41%) as fluorescent yellow oil. MS; m/z 292, 294 (M^+, $M^+ + 2$, based on ^{79}Br) for $C_{10}H_{14}BrNO_2S$. IR; 2955, 2930, and 2860 (CH), 1509 and 1326 (NO_2). ^{1}H NMR; 7.64 (1H, s, Th–H), 2.57 (2H, t, $J = 8$ Hz, $CH_2(CH_2)_4CH_3$), 1.65–1.20 (8H, m, $CH_2(CH_2)_4CH_3$), 0.90 (3H, t, $J = 7$ Hz, CH_3). UV–vis; 294 (4300), 346 (9600). Found: C, 40.83; H, 4.96; N, 4.85%. Calcd for $C_{10}H_{14}BrNO_2S$: C, 41.09; H, 4.83; N, 4.79%.

5-Bromo-5′-cyano-3,3′-dihexyl-2,2′-bithiophene (9c). 9c was prepared by way of Method B, similar to 2-bromo-5-cyano-3-hexylthiophene. The oximes **11** were separated to each isomer by column chromatography on SiO_2 with $CHCl_3$. Syn-oxime ($R_f = 0.14$ with $CHCl_3$) of **11**: Yield; 46%. Pale yellow semi-solid. MS; m/z 456, 458 ($M^+ + 1$, $M^+ + 3$, based on ^{79}Br) for $C_{21}H_{30}BrNOS_2$. IR; 3277 (br, OH), 2957, 2925, and 2870 (CH), 1631 (CNO), 1464 (NO). ^{1}H NMR; 8.20 (1H, s, HCNO), 7.64 (1H, s, OH), 7.23 (1H, s, Th–H), 7.05 (1H, s, Th–H), 2.52–2.44 (4H, m, $CH_2(CH_2)_4CH_3$), 1.52–1.22 (16H, m, $CH_2(CH_2)_4CH_3$), 0.88–0.83 (6H, m, CH_3). UV–vis; 308 (12880). Found: C, 54.96; H, 6.73; N, 3.11%. Calcd for $C_{21}H_{30}BrNOS_2$: C, 55.24; H, 6.62; N, 3.07%. Anti-oxime ($R_f = 0.35$ with $CHCl_3$) of **11**: Yield; 52%. Pale yellow semi-solid. MS; m/z 456, 458 ($M^+ + 1$, $M^+ + 3$, based on ^{79}Br) for $C_{21}H_{30}BrNOS_2$. IR; 3600–2900 (very br, OH), 2930, 2855, and 2870 (CH), 1649 (CNO), 1466 (NO). ^{1}H NMR; 8.20 (1H, s, HCNO), 7.64 (1H, br s, OH), 7.23 (1H, s, Th–H), 7.05 (1H, s, Th–H), 2.48–2.42 (4H, m, $CH_2(CH_2)_4CH_3$), 1.51–1.15 (16H, m, $CH_2(CH_2)_4CH_3$), 0.90–0.80 (6H, m, CH_3). UV–vis; 301 (13500). Found: C, 55.01; H, 6.90; N, 2.88%. Calcd for $C_{21}H_{30}BrNOS_2$: C, 55.24; H, 6.62; N, 3.07%. **9c**: Yield; 62% from the syn-oxime and 97% from the anti-oxime. Yellow semi-solid. MS; m/z 438, 440 ($M^+ + 1$, $M^+ + 3$, based on ^{79}Br) for $C_{21}H_{28}BrNS_2$. IR; 2955, 2927, and 2857 (CH), 2216 (CN). ^{1}H NMR; 7.47 (1H, s, Th–H), 6.96 (1H, s, Th–H), 2.49 (2H, t, $J = 8$ Hz, $CH_2(CH_2)_4CH_3$), 2.43 (2H, t, $J = 8$ Hz, $CH_2(CH_2)_4CH_3$), 1.55–1.20 (16H, m, $CH_2(CH_2)_4CH_3$), 0.88–0.85 (6H, m, CH_3). UV–vis; 252 (13600), 275 (11200, sh), 329 (9150). Found: C, 57.37; H, 6.66; N, 3.03%. Calcd for $C_{21}H_{28}BrNS_2$: C, 57.51; H, 6.44; N, 3.19%.

5-Bromo-5′-cyano-4,4′-dihexyl-2,2′-bithiophene (15c). 15c was prepared by way of Method B, similar to **9c**. Syn- and anti-oximes **13** from **15d** were distinguished from each other on TLC ($R_f = 0.12$ and 0.38 with $CHCl_3$) but could not be separated from each isomer. The extracts of the respective isomers from preparative TLC with $CHCl_3$ spontaneously changed, affording the same mixture of syn- and anti-oximes reproducibly. The ratio of syn- and anti-oximes could not be ascertained because there were no distinguishable peaks belonging to each isomer in ^{1}H NMR spectrum. Thus, the characterization of the product was determined as an equilibrium mixture. Yield; total 89%. Pale yellow semi-solid. MS; m/z 457, 459 ($M^+ + 1$, $M^+ + 3$, based on ^{79}Br) for $C_{21}H_{30}BrNOS_2$. IR; 3170, 3065 and 3020 together with a broad band at 3450–2750 (OH), 2952, 2926, and 2855 (CH), 1635 and 1618 (CNO), 1467 (br, NO). ^{1}H NMR; 8.29 (1H, s, HCNO), 7.75 (1H, br s, OH), 6.88 (1H, s, Th–H), 6.86 (1H, s, Th–H), 2.74–2.51 (4H, m, $CH_2(CH_2)_4CH_3$), 1.63–1.31 (16H, m, $CH_2(CH_2)_4CH_3$), 0.90–0.88 (6H, m, CH_3). UV–vis; 257 (6800), 353 (15300), 377 (10750, sh). Found: C, 55.18; H, 6.83; N, 3.33%. Calcd for $C_{21}H_{30}BrNOS_2$: C, 55.24; H, 6.62; N, 3.07%. **15c**: Yield; 97% from a mixture of syn- and anti-oximes. Yellow semi-solid. MS; m/z 439, 441 ($M^+ + 1$, $M^+ + 3$, based on ^{79}Br) for $C_{21}H_{28}BrNS_2$. IR; 2955, 2927, and 2857 (CH), 2216 (CN). ^{1}H NMR; 6.94 (1H, s, Th–H), 6.90 (1H, s, Th–H), 2.74 (2H, t, $J = 8$ Hz, $CH_2(CH_2)_4CH_3$), 2.54 (2H, t, $J = 8$ Hz, $CH_2(CH_2)_4$-

CH_3), 1.68–1.27 (16H, m, $CH_2(CH_2)_4CH_3$), 0.91–0.89 (6H, m, CH_3). UV–vis; 265 (6500), 341 (14800). Found: C, 57.29; H, 6.40; N, 3.12%. Calcd for $C_{21}H_{28}BrNS_2$: C, 57.51; H, 6.44; N, 3.19%.

5-Bromo-5′-formyl-3,3′-dihexyl-2,2′-bithiophene (9d). To a solution of **9b**[14] (2 g, 4.06 mmol) in THF (20 cm^3) was added *n*-BuLi (1.6 M solution in hexane, 2.53 cm^3, 4.05 mmol) dropwise at −78 °C over 15 min under Ar atmosphere and stirred for additional 20 min. To the resulting solution, DMF (1.57 cm^3, 20.3 mmol) was added at −78 °C and the mixture was gradually warmed up to room temperature. Poured into water, the reaction mixture was extracted with hexane. The extracts were washed with brine and then dried. The residue obtained after removal of the solvent was chromatographed on SiO_2 (3.8 × 11 cm) with hexane–$CHCl_3$ to afford **9d** (1.03 g, 57%) as pale yellow oil. **9d**: MS; *m*/*z* 441, 443 ($M^+ + 1$, $M^+ + 3$, based on ^{79}Br) for $C_{21}H_{29}BrOS_2$. IR; 2955, 2927, and 2857 (CH), 1675 (CO). ^{1}H NMR; 9.86 (1H, s, CHO), 7.63 (1H, s, Th–H), 6.96 (1H, s, Th–H), 2.54 (2H, t, $J = 8$ Hz, $CH_2(CH_2)_4CH_3$), 2.46 (2H, t, $J = 8$ Hz, $CH_2(CH_2)_4CH_3$), 1.60–1.25 (16H, m, $CH_2(CH_2)_4CH_3$), 0.95–0.80 (6H, m, CH_3). UV–vis; 264 (12500), 329 (9800). Found: C, 56.84; H, 6.90%. Calcd for $C_{21}H_{29}BrOS_2$: C, 57.12; H, 6.62%.

5-Bromo-5′-formyl-4,4′-dihexyl-2,2′-bithiophene (15d). This compound was prepared from **15b**[8,14] similar to **9d**. **15d**: Yield; 84%. Yellow oil. MS; *m*/*z* 441, 443 ($M^+ + 1$, $M^+ + 3$, based on ^{79}Br) for $C_{21}H_{29}BrOS_2$. IR; 2955, 2927, and 2857 (CH), 1655 (CO). ^{1}H NMR; 9.98 (1H, s, CHO), 7.02 (1H, s, Th–H), 6.97 (1H, s, Th–H), 2.91 (2H, t, $J = 8$ Hz, $CH_2(CH_2)_4CH_3$), 2.55 (2H, t, $J = 8$ Hz, $CH_2(CH_2)_4CH_3$), 1.75–1.20 (16H, m, $CH_2(CH_2)_4CH_3$), 0.95–0.80 (6H, m, CH_3). UV–vis; 263 (8800), 371 (22900). Found: C, 56.89; H, 6.48%. Calcd for $C_{21}H_{29}BrOS_2$: C, 57.12; H, 6.62%.

5-Bromo-3,3′-dihexyl-5′-nitro-2,2′-bithiophene (9e). To a solution of **9a**[14] (550 mg, 1.93 mmol) in Ac_2O (8 cm^3) was added a mixture of HNO_3 (60% solution, 1 cm^3, 9.5 mmol) and Ac_2O (4 cm^3) at −40 °C over 15 min under Ar atmosphere, and the mixture was kept standing at 0 °C for 12 h. A solution of KOH (2 M solution in H_2O, 60 cm^3) was added to the reaction mixture at 0 °C, and then after 30 min stirring the mixture was extracted with $CHCl_3$. The extracts were washed with brine and dried. The residue obtained after removal of the solvent was chromatographed on SiO_2 (3.2 × 8 cm) with hexane–$CHCl_3$ to **9e** (660 mg, quantitative) as yellow oil. MS; *m*/*z* 457, 459 (M^+, $M^+ + 2$, based on ^{79}Br) for $C_{20}H_{28}BrNO_2S_2$. IR; 2955, 2928, and 2857 (CH), 1508 and 1334 (NO_2). ^{1}H NMR; 7.79 (1H, s, Th–H), 7.08 (1H, s, Th–H), 2.50 (2H, t, $J = 8$ Hz, $CH_2(CH_2)_4CH_3$), 2.47 (2H, t, $J = 8$ Hz, $CH_2(CH_2)_4CH_3$), 1.57–1.21 (16H, m, $CH_2(CH_2)_4CH_3$), 0.88–0.84 (6H, m, CH_3). UV–vis; 271 (11300), 357 (14600). Found: C, 52.08; H, 6.44; N, 2.88%. Calcd for $C_{20}H_{28}BrNO_2S_2$: C, 52.38; H, 6.16; N, 3.06%.

5-Bromo-4,4′-dihexyl-5′-nitro-2,2′-bithiophene (15e). This compound was prepared from **15a**[8,14] similar to **9e**. **15e**: Yield; 55%. Yellow semi-solid. MS; *m*/*z* 457, 459 (M^+, $M^+ + 2$, based on ^{79}Br) for $C_{20}H_{28}BrNO_2S_2$. IR; 2952, 2927, and 2859 (CH), 1531 and 1318 (NO_2). ^{1}H NMR; 7.03 (1H, s, Th–H), 6.88 (1H, s, Th–H), 3.02 (2H, t, $J = 8$ Hz, $CH_2(CH_2)_4CH_3$), 2.56 (2H, t, $J = 8$ Hz, $CH_2(CH_2)_4CH_3$), 1.68–1.32 (6H, m, $CH_2(CH_2)_4CH_3$), 0.90 (6H, br t, $J = 7$ Hz, CH_3). UV–vis; 277 (11000), 402 (22600). Found: C, 52.11; H, 6.39; N, 2.79%. Calcd for $C_{20}H_{28}NO_2S_2Br$: C, 52.38; H, 6.16; N, 3.06%.

General Preparative Procedures for the HTh–X and DHBTh–X Acetylenes 12 and 16. To each solution of the corresponding bromo derivatives (4–5 mmol), copper(I) iodide (CuI, 0.1–0.15 mmol) and dichlorobis(triphenylphosphine)palladium (0.2–0.25 mmol) in diisopropylamine (15 cm^3) was added TMSA (equivalent to the bromo derivative) at room temperature under Ar atmosphere. The mixture was stirred at room temperature for 3–5 h, by checking the reaction progress with TLC. The reaction mixture was poured into water and extracted with $CHCl_3$. The residue obtained after removal of the solvent was chromatographed on SiO_2 (3.2 × 5–10 cm) with hexane–$CHCl_3$ to afford the TMS-protected acetylene derivative. Successively, each solution of the TMS-protected acetylene derivatives (3–5 mmol) in methanol–hexane (10 cm^3, 4:1 v/v) was stirred in the presence of anhydrous sodium carbonate (Na_2CO_3; 0.6–0.7 mmol) at room temperature for 3–5 h. Poured into water, the mixture was extracted with $CHCl_3$ and the extracts were washed with brine. The residue obtained after removal of the solvent was chromatographed on Al_2O_3 (3.2 × 5–10 cm) with hexane–$CHCl_3$ to yield the desired acetylene derivative, which was employed for the next coupling reaction in a preparative purity grade. Thus, elemental analyses of the terminal acetylenes **7**, **12**, and **16** were all abandoned.

5-Cyano-3-hexyl-2-(trimethylsilylethynyl)thiophene: Yield; 84%. Yellow oil. MS; *m*/*z* 289 (M^+) for $C_{16}H_{23}NSSi$. IR; 2959, 2929, and 2859 (CH), 2216 (CN), 2148 (C≡C). ^{1}H NMR; 7.33 (1H, s, Th–H), 2.66 (2H, t, $J = 8$ Hz, $CH_2(CH_2)_4CH_3$), 1.65–1.20 (8H, m, $CH_2(CH_2)_4CH_3$), 0.90 (3H, t, $J = 7$ Hz, CH_3), 0.26 (9H, s, $Si(CH_3)_3$). UV–vis; 268 (4300), 279 (5600), 304 (8900), 316 (8900). Found: C, 66.12; H, 8.28; N, 4.62%. Calcd for $C_{16}H_{23}NSSi$: C, 66.38; H, 8.01; N, 4.84%. **7c**: Yield; 64%. Yellow oil. MS; *m*/*z* 217 (M^+) for $C_{13}H_{15}NS$. IR; 3309 (C≡CH), 2955, 2927 and 2857 (CH), 2217 (CN), 2110 (C≡C). ^{1}H NMR; 7.36 (1H, s, Th–H), 3.58 (1H, s, CCH), 2.68 (2H, t, $J = 8$ Hz, $CH_2(CH_2)_4CH_3$), 1.65–1.20 (8H, m, $CH_2(CH_2)_4CH_3$), 0.89 (3H, t, $J = 7$ Hz, CH_3). UV–vis; 293 (4.8, as relative intensity), 306 (14.8).

5-Formyl-3-hexyl-2-(trimethylsilylethynyl)thiophene: Yield, 82%. Yellow oil. MS; *m*/*z* 292 (M^+) for $C_{16}H_{24}OSSi$. IR; 2958, 2928, and 2858 (CH), 2146 (C≡C), 1673 (CO). ^{1}H NMR; 9.80 (1H, s, CHO), 7.50 (1H, s, Th–H), 2.69 (2H, t, $J = 8$ Hz, $CH_2(CH_2)_4CH_3$), 1.70–1.20 (8H, m, $CH_2(CH_2)_4CH_3$), 0.89 (3H, t, $J = 7$ Hz, CH_3), 0.27 (9H, s, $Si(CH_3)_3$). UV–vis; 295 (6900), 338 (12300). Found: C, 65.48; H, 8.55%. Calcd for $C_{16}H_{24}OSSi$: C, 65.70; H, 8.27%. **7d**: Yield; 94%. Yellow oil. MS; *m*/*z* 220 (M^+) for $C_{13}H_{16}OS$. IR; 3292 (C≡CH), 2956, 2928, and 2858 (CH), 2105 (C≡C), 1675 (CO). ^{1}H NMR; 9.83 (1H, s, CHO), 7.53 (1H, s, Th–H), 3.67 (1H, s, CCH), 2.72 (2H, t, $J = 8$ Hz, $CH_2(CH_2)_4CH_3$), 1.70–1.25 (8H, m, $CH_2(CH_2)_4CH_3$), 0.89 (3H, t, $J = 7$ Hz, CH_3). UV–vis; 290 (9.3, as relative intensity), 326 (11).

3-Hexyl-5-nitro-2-(trimethylsilylethynyl)thiophene: Yield; 80%. Yellow oil. MS; *m*/*z* 309 (M^+) for $C_{15}H_{23}NO_2SSi$. IR; 2958, 2929, and 2858 (CH), 2148 (C≡C), 1508 and 1331 (NO_2). ^{1}H NMR; 7.67 (1H, s, Th–H), 2.66 (2H, t, $J = 8$ Hz, $CH_2(CH_2)_4CH_3$), 1.70–1.25 (8H, m, $CH_2(CH_2)_4CH_3$), 0.89 (3H, t, $J = 7$ Hz, CH_3), 0.27 (9H, s, $Si(CH_3)_3$). UV–vis; 313 (4900), 372 (13500). Found: C, 57.99; H, 7.60; N, 4.26%. Calcd for $C_{15}H_{23}NO_2SSi$: C, 58.21; H, 7.49; N, 4.53%. **7e**: Yield; 76%. Yellow oil. MS; *m*/*z* 237 (M^+) for $C_{12}H_{15}NO_2S$. IR; 3288 (C≡CH), 2956, 2928, and 2859 (CH), 2105 (C≡C), 1510 and 1333 (NO_2). ^{1}H NMR; 7.69 (1H, s, Th–H), 3.66 (1H, s, CCH), 2.68 (2H, t, $J = 8$ Hz, $CH_2(CH_2)_4CH_3$), 1.70–1.25 (8H, m, $CH_2(CH_2)_4CH_3$), 0.89 (3H, t, $J = 7$ Hz, CH_3). UV–vis; 308 (7.4, as relative intensity), 357 (13).

5-Cyano-3,3′-dihexyl-5′-(trimethylsilylethynyl)-2,2′-bithiophene: Yield; 90%. Yellow oil. MS; *m*/*z* 455, 456 (M^+, $M^+ + 1$) for $C_{26}H_{37}NS_2Si$. IR; 2957, 2928, and 2858 (CH), 2212

(CN), 2142 (C≡C). ^{1}H NMR; 7.47 (1H, s, Th–H), 7.12 (1H, s, Th–H), 2.49 (2H, t, $J = 8$ Hz, CH_2(CH$_2$)$_4$CH$_3$), 2.43 (2H, t, $J = 8$ Hz, CH_2(CH$_2$)$_4$CH$_3$), 1.56–1.23 (16H, m, CH$_2$(CH_2)$_4$CH$_3$), 0.86 (6H, br m, CH$_3$), 0.26 (9H, s, Si(CH$_3$)$_3$). UV–vis; 270 (7650, sh), 302 (12500). Found: C, 68.18; H, 8.43; N, 2.77%. Calcd for $C_{26}H_{37}NS_2Si$: C, 68.51; H, 8.18; N, 3.07%. Further trial for a satisfactory analysis of this compound was given up. **12c**: Yield; 75%. Yellow semi-solid. MS; m/z 383, 384, 385 (M^+, $M^+ + 1$, $M^+ + 2$) for $C_{23}H_{29}NS_2$. IR; 3311 (C≡CH), 2957, 2928, and 2858 (CH), 2215 (CN), 2135 (C≡C). ^{1}H NMR; 7.48 (1H, s, Th–H), 7.16 (1H, s, Th–H), 3.41 (1H, s, CCH), 2.50 (2H, t, $J = 8$ Hz, CH_2(CH$_2$)$_4$CH$_3$), 2.44 (2H, t, $J = 8$ Hz, CH_2(CH$_2$)$_4$CH$_3$), 1.54–1.18 (16H, m, CH$_2$(CH_2)$_4$CH$_3$), 0.88–0.84 (6H, m, CH$_3$). UV–vis; 308 (5.7, as relative intensity), 357 (10).

5-Cyano-4,4′-dihexyl-5′-(trimethylsilylethynyl)-2,2′-bithiophene: Yield; 95%. Yellow oil. MS; m/z 455, 456 (M^+, $M^+ + 1$) for $C_{26}H_{37}NS_2Si$. IR; 2957, 2928, and 2858 (CH), 2216 (CN), 2148 (C≡C). ^{1}H NMR; 6.97 (1H, s, Th–H), 6.94 (1H, s, Th–H), 2.77 (2H, t, $J = 8$ Hz, CH_2(CH$_2$)$_4$CH$_3$), 2.68 (2H, t, $J = 8$ Hz, CH_2(CH$_2$)$_4$CH$_3$), 1.67–1.27 (16H, m, CH$_2$(CH_2)$_4$CH$_3$), 0.89–0.86 (6H, m, CH$_3$). UV–vis; 356 (17600), 385 (10500, sh). Found: C, 68.33; H, 8.38; N, 2.83%. Calcd for $C_{26}H_{37}NS_2Si$. C, 68.51; H, 8.18; N, 3.07%. **16c**: Yield; 98%. Yellow needles (hexane–$CHCl_3$). Mp; 88–91 °C. MS; m/z 383, 384, 385 (M^+, $M^+ + 1$, $M^+ + 2$) for $C_{23}H_{29}NS_2$. IR; (C≡CH), 2956, 2929, and 2858 (CH), 2210 (CN), 2136 (C≡C). ^{1}H NMR; 7.00 (1H, s, Th–H), 6.97 (1H, s, Th–H), 3.56 (1H, s, CCH), 2.74 (2H, t, $J = 8$ Hz, CH_2(CH$_2$)$_4$CH$_3$), 2.67 (2H, t, $J = 8$ Hz, CH_2(CH$_2$)$_4$CH$_3$), 1.74–1.28 (16H, m, CH$_2$(CH_2)$_4$CH$_3$), 0.92 (6H, br m, CH$_3$). UV–vis; 347 (14800), 378 (16600).

5-Formyl-3,3′-dihexyl-5′-(trimethylsilylethynyl)-2,2′-bithiophene: Yield, 78%. Yellow oil. MS; m/z 458 (M^+) for $C_{26}H_{38}OS_2Si$. IR; 2957, 2928, and 2857 (CH), 2147 (C≡C), 1676 (CO). ^{1}H NMR; 9.86 (1H, s, CHO), 7.63 (1H, s, Th–H), 7.13 (1H, s, Th–H), 2.54 (2H, t, $J = 8$ Hz, CH_2(CH$_2$)$_4$CH$_3$), 2.46 (2H, t, $J = 8$ Hz, CH_2(CH$_2$)$_4$CH$_3$), 1.60–1.15 (16H, m, CH$_2$(CH_2)$_4$CH$_3$), 0.95–0.80 (6H, m, CH$_3$), 0.25 (9H, s, Si(CH$_3$)$_3$). UV–vis; 273 (15100), 298 (13700), 341 (13600). Found: C, 67.85; H, 8.34%. Calcd for $C_{26}H_{38}OS_2Si$. C, 68.06; H, 8.35%. **12d**: Yield, 98%. Yellow oil. MS; m/z 386, 387 (M^+, $M^+ + 1$) for $C_{23}H_{30}OS_2$. IR; 3309 (C≡CH), 2955, 2927, and 2857 (CH), 2133 (C≡C), 1673 (CO). ^{1}H NMR; 9.87 (1H, s, CHO), 7.64 (1H, s, Th–H), 7.16 (1H, s, Th–H), 3.41 (1H, s, CCH), 2.55 (2H, t, $J = 8$ Hz, CH_2(CH$_2$)$_4$CH$_3$), 2.47 (2H, t, $J = 8$ Hz, CH_2(CH$_2$)$_4$CH$_3$), 1.60–1.25 (16H, m, CH$_2$(CH_2)$_4$CH$_3$), 0.90–0.75 (6H, m, CH$_3$). UV–vis; 270 (8.5, as relative intensity), 334 (7.8).

5-Formyl-4,4′-dihexyl-5′-(trimethylsilylethynyl)-2,2′-bithiophene: Yield, 66%. Yellow oil. MS; m/z 458 (M^+) for $C_{26}H_{38}OS_2Si$. IR; 2957, 2928, and 2857 (CH), 2141 (C≡C), 1656 (CO). ^{1}H NMR; 9.98 (1H, s, CHO), 7.06 (1H, s, Th–H), 7.02 (1H, s, Th–H), 2.91 (2H, t, $J = 8$ Hz, CH_2(CH$_2$)$_4$CH$_3$), 2.66 (2H, t, $J = 8$ Hz, CH_2(CH$_2$)$_4$CH$_3$), 1.75–1.25 (16H, m, CH$_2$(CH_2)$_4$CH$_3$), 0.90 (6H, t, $J = 7$ Hz, CH$_3$), 0.26 (9H, s, Si(CH$_3$)$_3$). UV–vis; 282 (8000), 388 (22400). Found: C, 67.79; H, 8.47%. Calcd for $C_{26}H_{38}OS_2Si$: C, 68.06; H, 8.35%. **16d**: Yield, 95%. Yellow oil. MS; m/z 386, 387 (M^+, $M^+ + 1$) for $C_{23}H_{30}OS_2$. IR; 3308 (C≡CH), 2955, 2927, and 2857 (CH), 2120 (C≡C), 1652 (CO). ^{1}H NMR; 9.98 (1H, s, CHO), 7.08 (1H, s, Th–H), 7.03 (1H, s, Th–H), 3.56 (1H, s, CCH), 2.91 (2H, t, $J = 8$ Hz, CH_2(CH$_2$)$_4$CH$_3$), 2.67 (2H, t, $J = 8$ Hz, CH_2(CH$_2$)$_4$CH$_3$), 1.75–1.20 (16H, m, CH$_2$(CH_2)$_4$CH$_3$), 0.89 (6H, t, $J = 7$ Hz, CH$_3$). UV–vis; 276 (1.0 as relative intensity), 379 (3.1).

3,3′-Dihexyl-5-nitro-5′-(trimethylsilylethynyl)-2,2′-bithiophene: Yield, 98%. Yellow solid. MS; m/z 475, 476 (M^+, $M^+ + 1$) for $C_{25}H_{37}NO_2S_2Si$. IR; 2957, 2928, and 2858 (CH), 2148 (C≡C), 1508 and 1334 (NO$_2$). ^{1}H NMR; 7.79 (1H, s, Th–H), 7.12 (1H, s, Th–H), 2.50 (2H, t, $J = 8$ Hz, CH_2(CH$_2$)$_4$CH$_3$), 2.47 (2H, t, $J = 8$ Hz, CH_2(CH$_2$)$_4$CH$_3$), 1.53–1.23 (16H, m, CH$_2$(CH_2)$_4$CH$_3$), 0.90–0.84 (6H, m, CH$_3$), 0.25 (9H, s, Si(CH$_3$)$_3$). UV–vis; 287 (18100), 368 (13600). Found: C, 63.01; H, 7.94; N, 2.78%. Calcd for $C_{25}H_{37}NO_2S_2Si$: C, 63.11; H, 7.84; N, 2.94%. **12e**: Yield, quantitative. Yellow solid. MS; m/z 403, 404 (M^+, $M^+ + 1$) for $C_{22}H_{29}NO_2S_2$. IR; 3312 (C≡CH), 2956, 2928, and 2858 (CH), 2125 (C≡C), 1508 and 1335 (NO$_2$). ^{1}H NMR; 7.80 (1H, s, Th–H), 7.17 (1H, s, Th–H), 3.43 (1H, s, CCH), 2.52–2.46 (4H, m, CH_2(CH$_2$)$_4$CH$_3$), 1.57–1.19 (16H, m, CH$_2$(CH_2)$_4$CH$_3$), 0.88–0.85 (6H, m, CH$_3$). UV–vis; 280 (16800), 363 (12300).

4,4′-Dihexyl-5-nitro-5′-(trimethylsilylethynyl)-2,2′-bithiophene: Yield, 67%. Yellow oil. MS; m/z 475, 476 (M^+, $M^+ + 1$) for $C_{25}H_{37}NO_2S_2Si$. IR; 2956, 2929, and 2859 (CH), 2140 (C≡C), 1543 and 1321 (NO$_2$). ^{1}H NMR; 7.07 (1H, s, Th–H), 6.92 (1H, s, Th–H), 3.02 (2H, t, $J = 8$ Hz, CH_2(CH$_2$)$_4$CH$_3$), 2.66 (2H, t, $J = 8$ Hz, CH_2(CH$_2$)$_4$CH$_3$), 1.69–1.26 (16H, m, CH$_2$(CH_2)$_4$CH$_3$), 0.91–0.87 (6H, m, CH$_3$), 0.27 (9H, s, Si(CH$_3$)$_3$). UV–vis; 290 (8050), 416 (19400). Found: C, 63.00; H, 8.02; N, 2.76%. Calcd for $C_{25}H_{37}NO_2S_2Si$. C, 63.11; H, 7.84; N, 2.94%. **16e**: Yield, 95%. Yellow solid. MS; m/z 403, 404 (M^+, $M^+ + 1$) for $C_{22}H_{29}NO_2S_2$. IR; 3308 (C≡CH), 2956, 2929, and 2858 (CH), 2100 (C≡C), 1531 and 1318 (NO$_2$). ^{1}H NMR; 7.09 (1H, s, Th–H), 6.94 (1H, s, Th–H), 3.58 (1H, s, CCH), 3.02 (2H, t, $J = 8$ Hz, CH_2(CH$_2$)$_4$CH$_3$), 2.68 (2H, t, $J = 8$ Hz, CH_2(CH$_2$)$_4$CH$_3$), 1.68–1.31 (16H, m, CH$_2$(CH_2)$_4$CH$_3$), 0.91–0.88 (6H, m, CH$_3$). UV–vis; 289 (7700), 410 (18500).

General Coupling Procedures for the Title Compounds 1–4. To a solution of anhydrous Cu(OAc)$_2$ (7–10 mmol, more than 10 times to the total amount of corresponding acetylenes) in Py–MeOH (100 cm^3, 5:1 v/v), a mixture of OEP acetylene **5** (0.1–0.2 mmol) and DHBTh acetylene **12** or **16** (0.5–1.0 mmol, ca. 5 times to **5**) in Py–MeOH (250 cm^3, 5:1 v/v) was added at 40–45 °C over 12 h. The mixture was stirred at room temperature for additional 12 h, by checking the reaction progress with TLC. The reaction mixture was concentrated under reduced pressure to ca. 30 cm^3 in volume, poured into water and extracted with $CHCl_3$. The extracts were washed with dil. HCl, sat. NaHCO$_3$, brine, and then dried. The residue obtained after removal of the solvent was chromatographed on SiO$_2$ (3.8 × 30 cm) with hexane–$CHCl_3$ to afford the products **1**–**4**, together with the diacetylene-group connected OEP, Bzn, HTh, and DHBTh dimers **17**–**21** (Chart 2),[34] respectively. Among derivatives **1**–**4**, the new products are only shown.

1b: Yield; 77%. Reddish purple microcrystallines (hexane–$CHCl_3$). Mp; >260 °C. MS; m/z 793, 795 ($M^+ + 1$, $M^+ + 3$ based on ^{79}Br) for $C_{46}H_{47}BrN_4Ni$. IR; 2961, 2926, and 2866 (CH), 2200 and 2138 (C≡C). ^{1}H NMR; 9.42 (2H, s, meso-H), 9.40 (1H, s, meso-H), 7.51 and 7.47 (2H each, d, $J = 13$ Hz, Bzn–H), 4.13 (4H, q, $J = 8$ Hz, CH$_2$), 3.83–3.76 (12H, m, CH$_2$), 1.81–1.71 (24H, m, CH$_3$). UV–vis; 410 (56600, sh), 435 (130800), 588 (14500), 610 (9650). Found: C, 69.34; H, 6.18; N, 6.86%. Calcd for $C_{46}H_{47}BrN_4Ni$: C, 69.54; H, 5.96; N, 7.05%.

1c: Yield; 73%. Reddish purple microcrystallines (hexane–$CHCl_3$). Mp; 255–260 °C (dec). MS; m/z 739, 740 (M^+, $M^+ + 1$) for $C_{47}H_{47}N_5Ni$. IR; 2965, 2930, and 2870 (CH), 2227 (CN), 2193 and 2136 (C≡C). ^{1}H NMR; 9.43 (2H, s, meso-H), 9.41 (1H,

s, meso-H), 7.69 and 7.67 (2H each, d, $J = 13$ Hz, Bzn–H), 4.12 (4H, q, $J = 8$ Hz, CH_2), 3.83–3.76 (12H, m, CH_2), 1.81–1.72 (24H, m, CH_3). UV–vis; 440 (108000, sh), 446 (127700), 565 (86500, sh), 587 (11500), 607 (12050), 615 (9650, sh). Found: C, 76.12; H, 6.50; N, 9.46%. Calcd for $C_{47}H_{47}N_5Ni$: C, 76.22; H, 6.40; N, 9.46%.

1d: Yield; 66%. Reddish purple microcrystallines (hexane–$CHCl_3$). Mp; 260–267 °C (dec). MS; *m/z* 742, 743 (M^+, $M^+ + 1$) for $C_{47}H_{48}N_4NiO$. IR; 2963, 2930, and 2869 (CH), 2191 and 2136 (C≡C), 1699 (CO), 1598 (C=C). ^{1}H NMR; 10.05 (1H, s, CHO), 9.43 (2H, s, meso-H), 9.41 (1H, s, meso-H), 7.89 and 7.75 (2H each, d, $J = 13$ Hz, Bzn–H), 4.13 (4H, q, $J = 8$ Hz, CH_2CH_3), 3.84–3.75 (12H, m, CH_2), 1.83–1.71 (24H, m, CH_3). UV–vis; 445 (117000, sh), 450 (135500), 570 (10700, sh), 596 (11800), 615 (11000, sh). Found: C, 75.68; H, 6.43; N, 7.18%. Calcd for $C_{47}H_{48}N_4NiO$: C, 75.91; H, 6.51; N, 7.54%. Further trial for a satisfactory analysis of this compound was given up.

2c: Yield; 43%. Dark green microcrystallines ($CHCl_3$–MeOH). Mp; >280 °C. MS; *m/z* 830, 831 ($M^+ + 1$, $M^+ + 2$) for $C_{51}H_{57}N_5SNi$. IR; 2961, 2928, and 2869 (CH), 2209 (CN), 2181 and 2130 (C≡C). ^{1}H NMR; 9.43 (2H, s, meso-H), 9.41 (1H, s, meso-H), 7.40 (1H, s, Th–H), 4.11 (4H, q, $J = 8$ Hz, CH_2CH_3), 3.85–3.70 (12H, m, CH_2CH_3), 2.79 (2H, t, $J = 8$ Hz, $CH_2(CH_2)_4CH_3$), 1.85–1.65 (24H, m, CH_2CH_3), 1.40–1.20 (8H, m, $CH_2(CH_2)_4CH_3$), 0.90 (3H, t, $J = 7$ Hz, $CH_2(CH_2)_4CH_3$). UV–vis; 453 (94600), 580 (68000, sh), 595 (10700), 618 (9400, sh). Found: C, 73.56; H, 6.78; N, 8.27%. Calcd for $C_{51}H_{57}N_5NiS$: C, 73.73; H, 6.92; N, 8.43%.

2d: Yield; 27%. Dark green microcrystallines ($CHCl_3$–MeOH). Mp; >280 °C. MS; *m/z* 833, 834 ($M^+ + 1$, $M^+ + 2$) for $C_{51}H_{58}N_4NiOS$. IR; 2964, 2929, and 2870 (CH), 2178 and 2130 (C≡C), 1669 (CO). ^{1}H NMR; 9.85 (1H, s, CHO), 9.43 (2H, s, meso-H), 9.41 (1H, s, meso-H), 7.57 (1H, s, Th–H), 4.12 (4H, q, $J = 8$ Hz, CH_2CH_3), 3.85–3.70 (12H, m, CH_2CH_3), 2.82 (2H, t, $J = 8$ Hz, $CH_2(CH_2)_4CH_3$), 1.85–1.70 (24H, m, CH_2CH_3), 1.45–1.25 (8H, m, $CH_2(CH_2)_4CH_3$), 0.90 (3H, t, $J = 7$ Hz, $CH_2(CH_2)_4CH_3$). UV–vis; 400 (36000, sh), 440 (76300), 462 (87200), 565 (63000, sh), 595 (14300), 610 (11500, sh). Found: C, 73.18; H, 7.24; N, 6.66%. Calcd for $C_{51}H_{58}N_4NiOS$: C, 73.46; H, 7.01; N, 6.72%.

2e: Yield; 11%. Dark green microcrystallines ($CHCl_3$–MeOH). Mp; >280 °C. MS; *m/z* 850, 851 (M^+, $M^+ + 1$) for $C_{50}H_{57}N_5NiO_2S$. IR; 2959, 2928, and 2869 (CH), 2178 and 2130 (C≡C), 1466 and 1319 (NO_2). ^{1}H NMR; 9.43 (2H, s, meso-H), 9.41 (1H, s, meso-H), 7.74 (1H, s, Th–H), 4.11 (4H, q, $J = 8$ Hz, CH_2CH_3), 3.85–3.70 (12H, m, CH_2CH_3), 2.79 (2H, t, $J = 8$ Hz, $CH_2(CH_2)_4CH_3$), 1.85–1.65 (24H, m, CH_2CH_3), 1.45–1.20 (8H, m, $CH_2(CH_2)_4CH_3$), 0.90 (3H, t, $J = 7$ Hz, $CH_2(CH_2)_4CH_3$). UV–vis; 431 (70500), 479 (37200), 605 (17100). Found: C, 70.38; H, 6.98; N, 8.12%. Calcd for $C_{50}H_{57}N_5ONiO_2S$: C, 70.58; H, 6.75; N, 8.23%.

3c: Yield; 62%. Dark green microcrystallines ($CHCl_3$–MeOH). Mp; >280 °C. MS; *m/z* 997, 998 (M^+, $M^+ + 1$) for $C_{61}H_{71}N_5NiS_2$. IR; 2962, 2928, and 2869 (CH), 2214 (CN), 2183 and 2131 (C≡C). ^{1}H NMR; 9.43 (2H, s, meso-H), 9.41 (1H, s, meso-H), 7.50 (1H, s, Th–H), 7.30 (1H, s, Th–H), 4.11 (4H, q, $J = 8$ Hz, CH_2CH_3), 3.88–3.77 (12H, m, CH_2CH_3), 2.54 (2H, t, $J = 8$ Hz, $CH_2(CH_2)_4CH_3$), 2.49 (2H, t, $J = 8$ Hz, $CH_2(CH_2)_4CH_3$), 1.81–1.71 (24H, m, CH_2CH_3), 1.28–1.26 (8H, m, $CH_2(CH_2)_4CH_3$), 0.89–0.86 (6H, m, $CH_2(CH_2)_4CH_3$). UV–vis; 446 (110600), 567 (9700, sh), 586 (9900), 618 (9600, sh). Found: C, 73.29; H, 7.30; N, 6.83%. Calcd for $C_{61}H_{71}N_5NiS_2$: C, 73.48; H, 7.18; N, 7.03%.

3d: Yield; 77%. Dark green microcrystallines ($CHCl_3$–MeOH). Mp; >280 °C. MS; *m/z* 1000, 1001 ($M^+ + 1$, $M^+ + 2$) for $C_{61}H_{72}N_4NiOS_2$. IR; 2962, 2927, and 2868 (CH), 2181 and 2130 (C≡C), 1671 (CO). ^{1}H NMR; 9.88 (1H, s, CHO), 9.42 (2H, s, meso-H), 9.40 (1H, s, meso-H), 7.65 (1H, s, Th–H), 7.31 (1H, s, Th–H), 4.12 (4H, q, $J = 8$ Hz, CH_2CH_3), 3.85–3.70 (12H, m, CH_2CH_3), 2.59 (2H, t, $J = 8$ Hz, $CH_2(CH_2)_4CH_3$), 2.53 (2H, t, $J = 8$ Hz, $CH_2(CH_2)_4CH_3$), 1.85–1.70 (24H, m, CH_2CH_3), 1.35–1.20 (16H, m, $CH_2(CH_2)_4CH_3$), 0.90 (6H, m, $CH_2(CH_2)_4CH_3$). UV–vis; 446 (100200), 560 (8800, sh), 588 (12900), 618 (10800, sh). Found: C, 73.11; H, 7.48; N, 5.51%. Calcd for $C_{61}H_{72}N_4NiOS_2$: C, 73.26; H, 7.26; N, 5.60%.

3e: Yield; 42%. Dark green microcrystallines ($CHCl_3$–MeOH). Mp; >280 °C. MS; *m/z* 1017, 1018 (M^+, $M^+ + 1$) for $C_{60}H_{71}N_5NiO_2S_2$. IR; 2964, 2930, and 2870 (CH), 2183 and 2133 (C≡C), 1464 and 1329 (NO_2). ^{1}H NMR; 9.42 (2H, s, meso-H), 9.40 (1H, s, meso-H), 7.82 (1H, s, Th–H), 7.30 (1H, s, Th–H), 4.12 (4H, q, $J = 8$ Hz, CH_2CH_3), 3.83–3.77 (12H, m, CH_2CH_3), 2.56 (2H, t, $J = 8$ Hz, $CH_2(CH_2)_4CH_3$), 2.54 (2H, t, $J = 8$ Hz, $CH_2(CH_2)_4CH_3$), 1.81–1.72 (24H, m, CH_2CH_3), 1.28–1.23 (16H, m, $CH_2(CH_2)_4CH_3$), 0.89–86 (6H, m, $CH_2(CH_2)_4CH_3$). UV–vis; 444 (101500), 565 (22000, sh), 590 (32000), 610 (23500, sh). Found: C, 70.48; H, 7.34; N, 6.79%. Calcd for $C_{60}H_{71}N_5NiO_2S_2$: C, 70.85; H, 7.04; N, 6.89%. Further trial for a satisfactory analysis of this compound was given up.

4c: Yield; 65%. Dark green microcrystallines ($CHCl_3$–MeOH). Mp; 240–250 °C (dec). MS; *m/z* 997, 998 (M^+, $M^+ + 1$) for $C_{61}H_{71}N_5NiS_2$. IR; 2962, 2929, and 2869 (CH), 2206 (CN), 2173 and 2126 (C≡C). ^{1}H NMR; 9.42 (2H, s, meso-H), 9.39 (1H, s, meso-H), 7.07 (1H, s, Th–H), 7.01 (1H, s, Th–H), 4.12 (4H, q, $J = 8$ Hz, CH_2CH_3), 3.84–3.70 (12H, m, CH_2CH_3), 2.83–2.74 (4H, m, $CH_2(CH_2)_4CH_3$), 1.82–1.68 (24H, m, CH_2CH_3), 1.36–1.23 (8H, m, $CH_2(CH_2)_4CH_3$), 0.90 (6H, m, $CH_2(CH_2)_4CH_3$). UV–vis; 400 (23500, sh), 444 (100400, sh), 465 (132600), 565 (9450, sh), 593 (10800), 610 (8800, sh). Found: C, 73.27; H, 7.47; N, 6.78%. Calcd for $C_{61}H_{71}N_5NiS_2$: C, 73.48; H, 7.18; N, 7.03%.

4d: Yield; 55%. Dark green microcrystallines ($CHCl_3$–MeOH). Mp; >280 °C. MS; *m/z* 1000, 1001 ($M^+ + 1$, $M^+ + 2$) for $C_{61}H_{72}N_4NiOS_2$. IR; 2962, 2928, and 2868 (CH), 2183 and 2126 (C≡C), 1652 (CO). ^{1}H NMR; 9.99 (1H, s, CHO), 9.42 (2H, s, meso-H), 9.40 (1H, s, meso-H), 7.13 (1H, s, Th–H), 7.05 (1H, s, Th–H), 4.13 (4H, q, $J = 7$ Hz, CH_2CH_3), 3.85–3.70 (12H, m, CH_2CH_3), 2.91 (2H, t, $J = 8$ Hz, $CH_2(CH_2)_4CH_3$), 2.78 (2H, t, $J = 8$ Hz, $CH_2(CH_2)_4CH_3$), 1.85–1.65 (24H, m, CH_2CH_3), 1.45–1.20 (16H, m, $CH_2(CH_2)_4CH_3$), 0.90–0.85 (6H, m, $CH_2(CH_2)_4CH_3$). UV–vis; 402 (26500, sh), 451 (89100), 471 (95000), 568 (17000, sh), 596 (20200). Found: C, 73.12; H, 7.47; N, 5.33%. Calcd for $C_{61}H_{72}N_4NiOS_2$: C, 73.26; H, 7.26; N, 5.60%.

4e: Yield; 57%. Dark green microcrystallines ($CHCl_3$–MeOH). Mp; >280 °C. MS; *m/z* 1017, 1018 (M^+, $M^+ + 1$) for $C_{60}H_{71}N_5NiO_2S_2$. IR; 2963, 2929, and 2870 (CH), 2173 and 2128 (C≡C), 1464 and 1315 (NO_2). ^{1}H NMR; 9.42 (2H, s, meso-H), 9.40 (1H, s, meso-H), 7.15 (1H, s, Th–H), 6.98 (1H, s, Th–H), 4.13 (4H, q, $J = 8$ Hz, CH_2CH_3), 3.83–3.78 (12H, m, CH_2CH_3), 3.03 (2H, t, $J = 8$ Hz, $CH_2(CH_2)_4CH_3$), 2.79 (2H, t, $J = 8$ Hz, $CH_2(CH_2)_4CH_3$), 1.81–1.66 (24H, m, CH_2CH_3), 1.43–1.33 (16H, m, $CH_2(CH_2)_4CH_3$), 0.92–0.90 (6H, m, $CH_2(CH_2)_4CH_3$). UV–vis; 434 (771000, sh), 450 (78000), 493 (62600, sh), 599 (28000). Found: C, 70.58; H, 7.28; N, 6.64%. Calcd for $C_{60}H_{71}N_5NiO_2S_2$: C, 70.85; H, 7.04; N, 6.89%.

Financial support by a Grant-in-Aid for Scientific and Research from the Ministry of Education, Culture, Sports, Science and Technology, is gratefully acknowledged. The present work was financially supported in part by The Hokuriku Industrial Advancement Center (HIAC). HH also expresses his great appreciation to VBL Research Center and Center of Instrumental Analyses, University of Toyama, for their supporting measurements of the structural and physical properties of the new compounds.

References

This paper is dedicated to Emeritus Professor Philip Eaton on the occasion of his 70th birth year.

1 A part of this work was preliminarily reported: H. Imahori, H. Higuchi, Y. Matsuda, A. Itagaki, Y. Sakai, J. Ojima, Y. Sakata, *Bull. Chem. Soc. Jpn.* **1994**, *67*, 2500.

2 A part of this work was preliminarily reported: N. Hayashi, H. Nakashima, Y. Takayama, H. Higuchi, *Tetrahedron Lett.* **2003**, *44*, 5423.

3 Only a few articles are shown. a) G. B. Kistiakowsky, J. R. Ruhoff, H. A. Smith, W. E. Vaughan, *J. Am. Chem. Soc.* **1936**, *58*, 146; M. J. S. Dewar, *Pure Appl. Chem.* **1975**, *44*, 767. b) S. B. Bulgarevich, V. S. Bolotnikov, V. N. Scheinker, O. A. Osipov, A. D. Garnovskii, *Zh. Org. Khim.* **1976**, *12*, 197; S. B. Bulgarrevich, T. A. Yusman, O. A. Osipov, *Zh. Obshch. Khim.* **1984**, *54*, 1603. c) M. J. S. Dewar, *The Molecular Orbital Theory of Organic Chemistry*, McGraw-Hill, New York, **1969**; J. I. Aihara, *J. Am. Chem. Soc.* **1976**, *98*, 6840. d) I. Gutman, M. Milun, N. Trinajstic, *J. Am. Chem. Soc.* **1977**, *99*, 1692.

4 Only a few articles are shown. a) D. I. Schuster, P. Cheng, P. D. Jarowski, D. M. Guldi, C. P. Luo, L. Echegoyen, S. Pyo, A. R. Holzwarth, S. E. Braslavsky, R. M. Williams, G. Klihm, *J. Am. Chem. Soc.* **2004**, *126*, 7257. b) K. Tomizaki, A. B. Lysenko, M. Taniguchi, J. S. Lindsey, *Tetrahedron* **2004**, *60*, 2011. c) T. Nakamura, J. Ikemoto, M. Fujitsuka, Y. Araki, O. Ito, K. Takimiya, Y. Aso, T. Otsubo, *J. Phys. Chem. B* **2005**, *109*, 14365. d) M. J. Hodgson, V. V. Borovkov, Y. Inoue, D. P. Arnold, *J. Organomet. Chem.* **2006**, *691*, 2162. e) K. M. Kadish, L. Fremond, F. Burdet, L.-M. Barbe, C. P. Gros, R. Guilard, *J. Inorg. Biochem.* **2006**, *100*, 858. f) F. Hauke, S. Atalick, D. M. Guldi, A. Hirsh, *Tetrahedron* **2006**, *62*, 1923.

5 a) T. Sugiyama, T. Wada, H. Sasabe, *Synth. Met.* **1989**, *28*, 323. b) H. Okawa, H. Hattori, A. Yanase, Y. Kobayashi, A. Carter, M. Sekiya, A. Kaneko, T. Wada, A. Yamada, H. Sasabe, *Mol. Cryst. Liq. Cryst.* **1992**, *B3*, 169. c) N. Hayashi, H. Nishi, K. Morizumi, I. Kobayashi, H. Sakai, R. Akaike, K. Tani, H. Higuchi, *Recent Res. Dev. Org. Chem.* **2004**, *8*, 401.

6 a) J. Casado, L. L. Miller, K. R. Mann, T. M. Pappenfus, H. Higuchi, E. Orti, B. Milian, R. Pou-Amerigo, V. Hernandez, J. T. Lopez Navarrete, *J. Am. Chem. Soc.* **2002**, *124*, 12380. b) D. E. Janzen, M. W. Burand, P. C. Ewbank, T. M. Pappenfus, H. Higuchi, D. A. da Silva Filho, V. G. Young, J.-L. Brédas, K. R. Mann, *J. Am. Chem. Soc.* **2004**, *126*, 15295.

7 a) F. Forster, in *Organic Chemistry, A Series of Monographs*, ed. by A. T. Blomquist, Academic Press, New York, **1969**, Vol. 15, p. 33. b) A. M. Moran, M. B. Desce, A. M. Kelley, *Chem. Phys. Lett.* **2002**, *358*, 320. c) U. Lawrentz, W. Grahn, K. Lukasznk, C. Klein, R. Wortmann, A. Feldner, D. Scherer, *Chem. Eur. J.* **2002**, *8*, 1573. d) A. C. Benniston, A. Harriman, P. Li, P. V. Patel, C. A. Sams, *J. Org. Chem.* **2006**, *71*, 3481, and many other references cited therein.

8 a) T. Wada, L. Wang, D. Fichou, H. Higuchi, J. Ojima, H. Sasabe, *Mol. Cryst. Liq. Cryst.* **1994**, *B255*, 149. b) H. Higuchi, Y. Uraki, H. Yokota, H. Koyama, J. Ojima, T. Wada, H. Sasabe, *Bull. Chem. Soc. Jpn.* **1998**, *71*, 483.

9 a) H. Higuchi, T. Ishikura, K. Miyabayashi, M. Miyake, K. Yamamoto, *Tetrahedron Lett.* **1999**, *40*, 9091. b) N. Hayashi, T. Matsukihira, K. Miyabayashi, M. Miyake, H. Higuchi, *Tetrahedron Lett.* **2006**, *47*, 5585.

10 a) H. Higuchi, T. Ishikura, K. Mori, Y. Takayama, K. Yamamoto, K. Tani, K. Miyabayashi, M. Miyake, *Bull. Chem. Soc. Jpn.* **2001**, *74*, 889. b) N. Hayashi, A. Matsuda, E. Chikamatsu, K. Mori, H. Higuchi, *Tetrahedron Lett.* **2003**, *44*, 7155.

11 G. Eglington, A. R. Galbraith, *Chem. Ind.* **1956**, 737.

12 K. Sonogashira, Y. Tohda, N. Hagihara, *Tetrahedron Lett.* **1975**, *16*, 4467.

13 S. Gronowitz, *Thiophene and Its Derivatives*, John Wiley and Sons, New York, **1992**.

14 a) H. Higuchi, T. Nakayama, H. Koyama, J. Ojima, T. Wada, H. Sasabe, *Bull. Chem. Soc. Jpn.* **1995**, *68*, 2363. b) H. Higuchi, H. Koyama, N. Hayashi, J. Ojima, T. Wada, H. Sasabe, *Nonlinear Opt.* **1996**, *15*, 209.

15 J. Nakayama, T. Fujimori, *Sulfur Lett.* **1990**, *11*, 29.

16 R. M. Kellogg, A. P. Schaap, E. T. Harper, H. Wynberg, *J. Org. Chem.* **1968**, *33*, 2902.

17 M. F. Browne, R. L. Shriner, *J. Org. Chem.* **1957**, *22*, 1320.

18 N. Hayashi, A. Naoe, K. Miyabayashi, M. Miyake, H. Higuchi, *Tetrahedron Lett.* **2005**, *46*, 6961.

19 P. L. Corio, B. P. Dailey, *J. Am. Chem. Soc.* **1956**, *78*, 3043.

20 a) S. Gronowitz, R. A. Hoffman, *Ark. Kemi* **1961**, *16*, 539. b) T. J. Batterham, in *NMR Spectra of Simple Heterocycles*, ed. by E. C. Taylor, A. Weissberger, John Wiley Sons, New York, **1973**, p. 423.

21 a) J. A. Pople, *Proc. R. Soc. London, Ser. A* **1957**, *239*, 541. b) J. S. Waugh, R. W. Fessenden, *J. Am. Chem. Soc.* **1957**, *79*, 846.

22 J. Kao, L. Radom, *J. Am. Chem. Soc.* **1979**, *101*, 311.

23 N. Hayashi, M. Murayama, K. Mori, A. Matsuda, E. Chikamatsu, K. Tani, K. Miyabayashi, M. Miyake, H. Higuchi, *Tetrahedron* **2004**, *60*, 6363.

24 J. W. Buchler, L. Puppe, *Liebigs Ann. Chem.* **1970**, 142.

25 H. Imahori, Y. Tanaka, T. Okada, Y. Sakata, *Chem. Lett.* **1993**, 1215.

26 W. T. Simpson, *J. Chem. Phys.* **1949**, *17*, 1218.

27 H. Higuchi, H. Koyama, H. Yokota, J. Ojima, *Tetrahedron Lett.* **1996**, *37*, 1617.

28 C. N. R. Rao, *Chem. Ind.* **1957**, 1239.

29 K. K. Baldridge, M. S. Gordon, *J. Am. Chem. Soc.* **1988**, *110*, 4204.

30 J. Deisenhofer, O. Epp, K. Miki, R. Huber, H. Michel, *J. Mol. Biol.* **1984**, *180*, 385.

31 H. Higuchi, K. Shimizu, M. Takeuchi, J. Ojima, K. Sugiura, Y. Sakata, *Bull. Chem. Soc. Jpn.* **1997**, *70*, 1923.

32 a) J.-H. Fuhrhop, in *Porphyrins and Metalloporphyrins*, ed. K. M. Smith, Elsevier Scientific Publishing Co., Netherlands, **1975**, p. 593. b) M. Gouterman, in *The Porphyrins*, ed. by D. Dolphin, Academic Press, New York, **1978**, Vol. III, p. 1. c) G. Loew, in *Inorganic Electronic Structure and Spectroscopy*, ed. by E. I. Solomon, A. B. P. Lever, John Wiley & Sons, Inc., New York, **1999**, Vol. II, p. 451.

33 a) H. Higuchi, S. Yoshida, Y. Uraki, J. Ojima, *Bull. Chem. Soc. Jpn.* **1998**, *71*, 2229. b) V. Hernández, S. Calvo Losada, J. Casado, H. Higuchi, J. T. López Navarrete, *J. Phys. Chem. A* **2000**, *104*, 661.

34 The synthetic strategy shown in the present work is not suitable for the synthesis of the derivatives **26** with TH orientation of DHBTh. Thus, the study to find new synthetic strategy for **26** is now underway. The synthetic success of **26** should enable us discuss conclusively about the substituent effect on not only oxidation potentials but also reduction potentials of the OEP derivatives. The substituent effect on the electronic properties of all the OEP derivatives including **26** will be reported continuously, as compared with the orientation effect of DHBTh.